SAPK/JNK activation by UV irradiation and Fcε-receptor stimulation was also attenuated in the *mkk7*$^{-/-}$ mast cells. Despite the impaired SAPK/JNK activation in the *mkk7*$^{-/-}$ cells, the expression of SEK1 was strongly up-regulated, and SEK1 protein was phosphorylated upon stimulation (11). Thus, both SEK1 and MKK7 seem to be required for the synergistic and functional activation of SAPK/JNK in a variety of mammalian cells.

To reveal the molecular mechanism of the synergistic activation of SAPK/JNK by SEK1 and MKK7 in living cells, we generated *mkk7*$^{-/-}$ mouse ES cells by gene targeting, in addition to *sek1*$^{-/-}$ ES cells, and further investigated the contribution of SEK1 and MKK7 to the activation and phosphorylation of the MAPK. Our present results clearly show that both SEK1 and MKK7 are required for the synergistic activation of SAPK/JNK in response to various stimuli in ES cells. Furthermore, we propose a sequential phosphorylation mechanism of SAPK/JNK by the two activators, SEK1 and MKK7, in the stress-stimulated living cells.

EXPERIMENTAL PROCEDURES

Generation of MKK7-deficient ES Cells—A 17-kbp DNA fragment of *mkk7* gene was isolated from a genomic 129/J mouse library. Targeting vector 1 contained a 585-bp short arm, a 6.7-kbp long arm, three loxP sequences, and a hygromycin resistance cassette (Hyg) in antisense orientation to *mkk7* transcription. Targeting vector 2 contained a 709-bp short arm, a 5.2-kbp long arm, and a neomycin resistance cassette (Neo) in antisense orientation to *mkk7* transcription. The linearized targeting vector 1 was electroporated into E14K ES cells. ES cell colonies resistant to hygromycin (0.2 mg/ml; Invitrogen) were screened for homologous recombination by PCR (30 s at 94 °C, 30 s at 60 °C, 1 min at 72 °C, for 40 cycles) using primers specific for *mkk7* genomic sequences and Hyg as described below. Next, the *mkk7*$^{+/hyg}$ ES cells were transfected with Cre recombinase expression vector, and cell colonies sensitive to hygromycin were screened for deletion of the region containing exons 4–13 and Hyg by PCR. The linearized targeting vector 2 was electroporated into *mkk7*$^{+/del}$ ES cells. Retargeted ES cell colonies resistant to G418 (0.3 mg/ml; Invitrogen) were screened for homologous recombination by PCR using primers specific for *mkk7* genomic sequences and Neo as described below. As a result, two *mkk7*$^{neo/del}$ clones (001 and 002) were independently obtained. Both clones lack MKK7 completely, and they are henceforth referred to as *mkk7*$^{-/-}$ ES cells in this manuscript. Specific primer sets used were 5′-GCC AAA ACA CGG AGT GCT GG-3′ and 5′-ATG TGA CCA GGC AGG AGT GG-3′ for wild-type (+) allele, 5′-TTA AGG CAA CTG GCA GAG-3′ and 5′-AGC TGA CTC TAG AGC TTG-3′ for hyg allele, 5′-ATC TGC CTG TAG CAT GCC-3′ and 5′-ACT CCA AAC ACC TCC CAC-3′ for del allele, 5′-GGA TGT GGA ATG TGT GCG AG-3′ and 5′-AGC TGG AAC CAC GCG CAA TGT GAG-3′ for neo allele. Recombinant ES cell clones were confirmed by Southern blotting of *Xba*I-digested genomic DNA hybridized to a 530-bp 3′-flanking probe.

Plasmids—Plasmids that express FLAG-tagged SEK1, MKK7γ2, and HA-tagged JNK1 were constructed as described previously (10). The cDNA encoding FLAG-tagged SEK1 kinase dominant-negative mutant (dnSEK1) by substituting Lys-129 with Arg (K129R) was cloned into mammalian expression vector pCMV5. The cDNAs encoding SAPK/JNK1 mutants Ala-Pro-Phe (APF), Ala-Pro-Tyr (APY), and Thr-Pro-Phe (TPF), were constructed by Kunkel method using the following three primers: 5′-GGA ACG AGT TTT ATG ATG GCG CCT TTT GTA GTG ACT CGC TAC TAC AGA GCA CC-3′ for APF mutant, 5′-GGA ACG AGT TTT ATG ATG GCG CCT TAT GTA GTG ACT CGC TAC TAC AGA GCA CC-3′ for APY mutant, and 5′-GGA ACG AGT TTT ATG ATG ACG CCT TTT GTA GTG ACT CGC TAC TAC AGA GCA CC-3′ for TPF mutant.

Antibodies—Antibodies against SAPK/JNK1 (C-17 and FL), MKK7/MEK7 (T-19), and SEK1/MEK4 (C-20) were purchased from Santa Cruz Biotechnology, Inc. Anti-phospho-SAPK/JNK (9251), and anti-phospho-SEK1 (9151) Abs were from Cell Signaling Technology. Anti-phospho-Tyr (PY20) and anti-phospho-Thr-Pro (P-Thr-Pro-101) mAbs were from BD Transduction Laboratories and Cell Signaling Technology, respectively. Anti-FLAG (M2) Ab and anti-HA affinity matrix were purchased from Sigma-Aldrich Co. and Roche Diagnostics, respectively. Rat anti-SEK1 (KN-001) and anti-MKK7 (KN-004) mAbs applicable to immunoprecipitation and immunoblotting were prepared in our laboratory as described previously (10).

Transfection—ES cells were plated at 2×10^6 cells onto a 60-mm dish and transfected 1 day later with 8 μg of plasmid DNA using LipofectAMINE 2000 (Invitrogen). The cells, after being cultured for 1 day, were transferred to four 35-mm dishes and cultured for another day. Human embryonic kidney 293T cells were plated at 1×10^6 cells onto a 35-mm dish and transfected 1 day later with 4 μg of plasmid DNA using LipofectAMINE 2000 (Invitrogen). The cells were stimulated and subjected for the assays of SAPK/JNK activity, immunoprecipitation, and immunoblotting.

Assay of SAPK/JNK Activity—ES cells were plated at 1.5×10^6 cells per 35-mm dish and cultured overnight. As chemical and physical stresses, the cells were stimulated by sorbitol (0.5 M; Wako), anisomycin (3 μg/ml; Sigma), nocodazole (0.5 μg/ml for 1 h; Sigma), UV light (1 kJ/m^2), and heat shock (44 °C for 10 min). SAPK/JNK proteins were immunoprecipitated at 4 °C for 2 h using the anti-SAPK/JNK polyclonal Ab (C-17; Santa Cruz Biotechnology, Inc.). The SAPK/JNK activity in the precipitated fractions was measured with glutathione *S*-transferase-c-Jun as an *in vitro* substrate in the presence of 60 μM [γ-^{32}P]ATP as described previously (12, 13).

Immunoprecipitarion and Immunoblotting—To detect the phosphorylation of Tyr and Thr residues in the Thr-Pro-Tyr motif of endogenous SAPK/JNK, ES cells were plated at ~2×10^7 cells onto a 150-mm dish and mixed with 2 ml of a lysis buffer (20 mM HEPES, pH 7.4, 1% Nonidet P-40, 10 mM NaCl, 0.05% 2-mercaptoethanol, 5 mM EDTA, 0.1 mM phenylmethylsulphonyl fluoride, 100 μM Na_3VO_4, 20 μg/ml of leupeptin, 50 mM NaF, and 1 mM benzamidine). The cell lysates were incubated with anti-SAPK/JNK Ab and protein A-Sepharose (Pharmacia) at 4 °C for 2 h, and the immuno-complexes were washed several times with the lysis buffer. The samples were analyzed by SDS-PAGE and immunoblotting. Proteins were electrophoretically transferred to a polyvinylidene difluoride membrane (Bio-Rad) and probed with anti-phospho-Tyr, phospho-Thr, and SAPK/JNK Abs. The bands were visualized by SuperSignal West Pico chemiluminescent substrate for the development of immunoblots using a horseradish peroxidase-conjugated second Ab according the manufacturer's instructions (Pierce). Endogenous SEK1 and MKK7 were immunoprecipitated with anti-SEK1 (KN-001) and anti-MKK7 (KN-004) mAbs and detected with anti-SEK1 (C-20) and anti-MKK7 (T-19) Abs, respectively.

All experiments were repeated at least three times with different batches of the cell samples, and the results were fully reproducible. Hence, most of the data shown are representative of several independent experiments.

RESULTS

Generation of MKK7-deficient ES Cells—To examine the role of MKK7 in SAPK/JNK regulation, we generated *mkk7*$^{-/-}$ ES cells using two targeting vectors in the process of *mkk7*$^{+/+}$, *mkk7*$^{+/hyg}$, *mkk7*$^{+/del}$, and *mkk7*$^{neo/del}$ construction as follows (Fig. 1). First, the exons 4–13 region of *mkk7* gene was deleted from one allele using targeting vector 1 and Cre recombinase (Fig. 1*A*). Second, another allele of *mkk7* was disrupted by replacing the site of activating phosphorylation in exon 9 with neomycin resistance cassette using targeting vector 2 (Fig. 1*B*). As a result, two clones (001 and 002) of *mkk7*$^{neo/del}$ ES cells that completely lack 48-kDa MKK7 were independently obtained (Fig. 1, *C* and *D*). Thus, the null-mutant *mkk7*$^{neo/del}$ clones are used as *mkk7*$^{-/-}$ ES cells in this study.

Impaired Stress-induced SAPK/JNK Activation in MKK7-deficient ES Cells—To examine the role of MKK7 in stress-induced activation of SAPK/JNK, *mkk7*$^{-/-}$ ES cells were incubated under various conditions, together with *sek1*$^{-/-}$and wild-type cells. Fig. 2 shows the time courses of SAPK/JNK activity in response to a protein synthesis inhibitor (*A*, 3 μg/ml of anisomycin), heat shock (*B*, 44 °C for 10 min), UV irradiation (*C*, 1 kJ/m^2), and hyperosmolar stress (*D*, 0.5 M sorbitol) in the two MAPKK mutant and wild-type ES cells. These stresses markedly stimulated SAPK/JNK activity in wild-type ES cells. Such stimulation, however, was severely impaired in both MAPKK mutant cells, although the cells contained SAPK/JNK at the same level as wild-type cells (see Fig. 4*C*). Thus, the stress-induced full activation of SAPK/JNK seems to require both SEK1 and MKK7 in ES cells.

The impairment of SAPK/JNK activation observed in the two

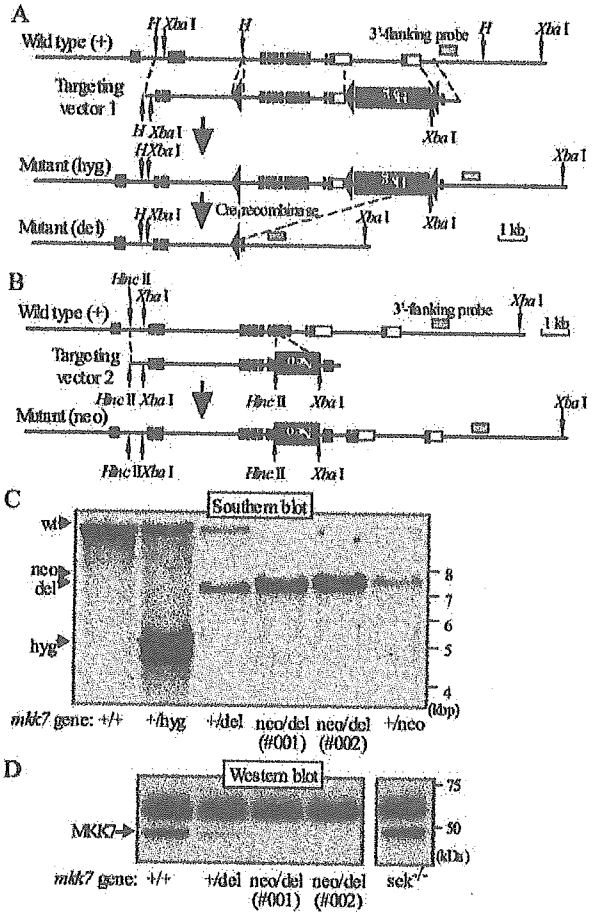

FIG. 1. **Targeted gene disruption of murine mkk7.** *A* and *B*, partial restriction map of murine genomic *mkk7* sequences and construction of targeting vectors 1 and 2. Targeting vector 1 (*A*) and 2 (*B*) contain a hygromycin resistance gene (Hyg) *plus* three loxP sequences (*triangles*) and a neomycin resistance gene (Neo), respectively. The 14 exons of *mkk7* are shown as *boxes*, and MKK7-coding regions as *filled boxes*. The genomic *mkk7* 3′-flanking probe used for Southern blotting is indicated as *gray boxes*. The predicted structures of targeted alleles are shown as *hyg*, *del*, and *neo*, respectively. Restriction enzymes used for the vector construction (*H*, *Hin*dIII, and *Hin*cII) and genomic Southern blotting (*Xba*I) are indicated by *arrows*. *C*, genomic analysis of ES cells. Genomic DNAs isolated from wild-type $mkk7^{+/+}$, $mkk7^{+/hyg}$, $mkk7^{+/del}$, $mkk7^{+/neo}$, and $mkk7^{neo/del}$ E14K ES cells were digested with *Xba*I and analyzed by Southern blotting using the 3′-flanking probe. Molecular weight markers and *mkk7* alleles (*wt*, 13 kb; *hyg*, 5 kb; *del*, 7.3 kb; *neo*, 7.8 kb) are indicated by *bars* and *arrows*, respectively. *D*, Western blot analysis of 48-kDa MKK7 in ES cells. MKK7 was immunoprecipitated and immunoblotted with anti-MKK7 mAb and polyclonal Ab, respectively. The position of 48-kDa MKK7 is indicated by an *arrow*. No MKK7 was detected in the two independent clones of $mkk7^{neo/del}$ ES cells (001 and 002). The amount of MKK7 in $sek1^{-/-}$ ES cells was comparable with that in wild-type cells.

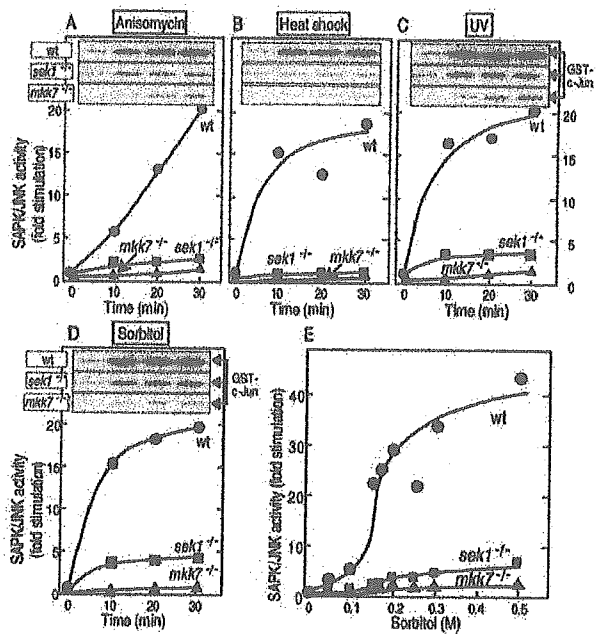

FIG. 2. **Time courses of stress-induced activation of SAPK/JNK in wild-type, $sek1^{-/-}$, and $mkk7^{-/-}$ ES cells.** Wild-type, $sek1^{-/-}$, and $mkk7^{-/-}$ ES cells were stimulated with anisomycin (*A*, 3 μg/ml), heat shock (*B*, 44 °C for 10 min), UV (*C*, 1 kJ/m²) or sorbitol (*D*, 0.5 M and *E*, the indicated concentrations) for the indicated times or 30 min (*E*). Cell lysates were prepared from the stimulated cells and immunoprecipitated with an anti-SAPK/JNK (C-17) Ab. SAPK/JNK activity in the precipitated fractions was measured with glutathione *S*-transferase-c-Jun as a substrate in the presence of [γ-^{32}P]ATP as described under "Experimental Procedures." The *insets* of *A–D* show the ^{32}P-phosphorylated glutathione *S*-transferase-c-Jun, and the activity is expressed as the -fold stimulation compared with the control level observed in wild-type ES cells without the stress. The data shown are representative of three independent experiments.

MAPKK mutant cells was further investigated with the different concentrations of sorbitol. As shown in Fig. 2*E*, the concentration-dependent activation curve of SAPK/JNK had a very steep upstroke at ~0.15 M sorbitol in wild-type ES cells. Interestingly, such steep activation of SAPK/JNK was markedly attenuated in $mkk7^{-/-}$ and $sek1^{-/-}$ ES cells without significant change in the half-maximum effective concentration of sorbitol. Impairment of SAPK/JNK activation in the two MAPKK mutant cells was also observed in other stress signals, including a microtubule-disruptive reagent, nocodazole, and genotoxic stresses, such as etoposide and arabinofuranosyl-cytosine (data not shown).

SEK1 and MKK7 Are Indispensable for Stress-induced SAPK/JNK Activation in ES Cells—The above results in Fig. 2 suggest that SEK1 and MKK7 synergistically contribute in the stress-induced stimulation of SAPK/JNK in ES cells. To elucidate the qualitative difference of the two MAPKKs, SEK1 and MKK7 expression vectors were transfected into $sek1^{-/-}$ or $mkk7^{-/-}$ ES cells (Fig. 3). SEK1 could rescue the impaired SAPK/JNK activation in response to UV irradiation and heat shock in $sek1^{-/-}$ ES cells (Fig. 3*A*). However, MKK7 isoforms α1, γ1, and γ2, could not restore the SAPK/JNK activation in $sek1^{-/-}$ ES cells. On the other hand, MKK7 α1 and γ1, but not SEK1, could rescue the impaired SAPK/JNK activation in response to heat shock, anisomycin, and nocodazole in $mkk7^{-/-}$ ES cells (Fig. 3*B*). These results clearly show that SEK1 and MKK7 serve different functions in the stress-induced SAPK/JNK activation in ES cells.

Properties of SEK1- and MKK7-induced Phosphorylation of SAPK/JNK—It has recently been reported that the phosphorylation of Thr and Tyr residues in the Thr-Pro-Tyr motif of SAPK/JNK is required for the full activation of the MAPK and that SEK1 and MKK7 preferentially phosphorylate the Tyr and Thr residues, respectively, *in vitro* (7–9). Therefore, we examined the stress-induced phosphorylation state of endogenous SAPK/JNK in $sek1^{-/-}$ and $mkk7^{-/-}$ ES cells together with wild-type cells. The three cell types were stimulated with 0.5 M of sorbitol (Fig. 4, *lanes 2*, *6*, and *10*), 1 kJ/m² of UV irradiation (*lanes 3*, *7*, and *11*), and 3 μg/ml of anisomycin (*lanes 4*, *8*, and

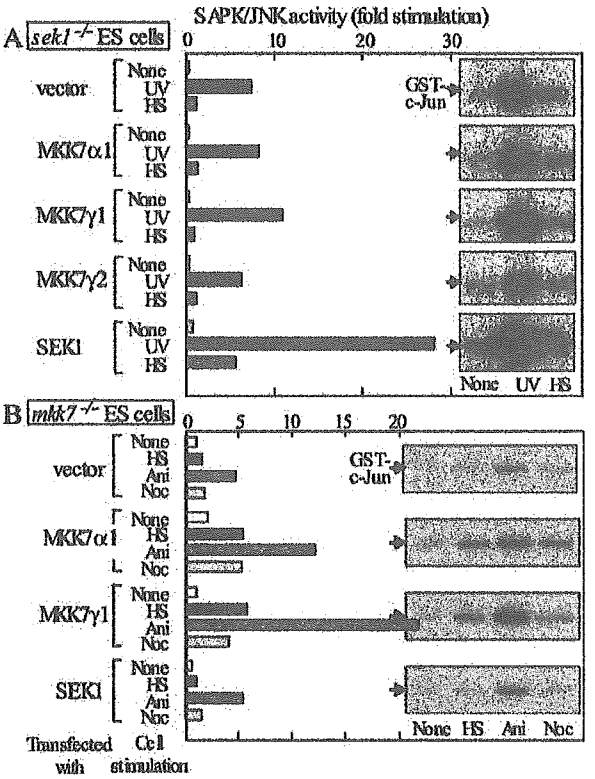

FIG. 3. **Effects of SEK1 or MKK7 expression on stress-induced SAPK/JNK activation in *sek1*$^{-/-}$ and *mkk7*$^{-/-}$ ES cells.** The two mutant *sek1*$^{-/-}$ (*A*) and *mkk7*$^{-/-}$ ES cells (*B*) were transfected with MKK7α1, γ1, γ2, or SEK1 expression vector. The transfected ES cells, after being cultured for 24 h, were stimulated with UV (1 kJ/m^2 and further incubation for 25 min), heat shock (*HS*, 43 °C for 30 min), anisomycin (*Ani*, 10 μg/ml for 30 min), or nocodazole (*Noc*, 0.5 μg/ml for 1 h). Cell lysates were prepared and immunoprecipitated with an anti-SAPK/JNK (C-17) Ab. SAPK/JNK activity in the precipitated fractions was measured as described in Fig. 2.

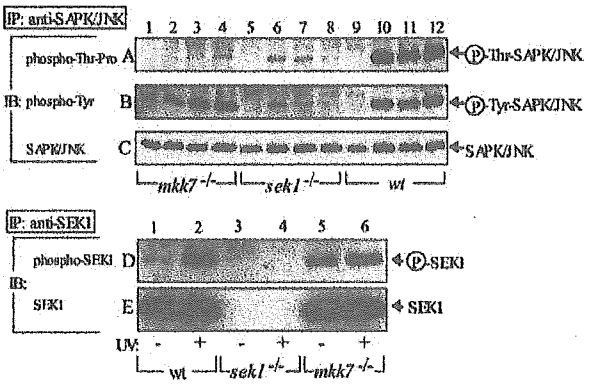

FIG. 4. **Stress-induced Thr and Tyr phosphorylation of endogenous SAPK/JNK in wild-type, *sek1*$^{-/-}$, and *mkk7*$^{-/-}$ ES cells.** ES cells were stimulated with 0.5 M sorbitol (*lanes 2, 6, 10*), 1 kJ/m^2 of UV irradiation (*lanes 3, 7, 11*), and 3 μg/ml of anisomycin (*lanes 4, 8, 12*) and further incubated at 37 °C for 25 min. Cell lysates were prepared, and endogenous SAPK/JNK and SEK1 were immunoprecipitated (*IP*) with anti-SAPK/JNK (C-17) polyclonal Abs (*A–C*) and anti-SEK1 (KN-001) mAb (*D* and *E*), respectively. The Thr phosphorylation (*A*) and Tyr phosphorylation (*B*) of SAPK/JNK, together with phosphorylated SEK1 (*D*) were determined using anti-phospho Abs as described under "Experimental Procedures." *IB*, immunoblots.

12). The endogenous SAPK/JNK was immunoprecipitated and analyzed by immunoblotting with phospho-specific Abs. In a series of the present experiments, these ES cells expressed almost the same amounts of SAPK/JNK (Fig. 4*C*). The existence of stress-induced Thr and Tyr phosphorylation within the Thr-Pro-Tyr motif of SAPK/JNK in wild-type cells could be detected with anti-phospho-Thr-Pro and anti-phospho-Tyr Abs, respectively (Fig. 4, *A* and *B*, *lanes 10–12*). Interestingly, Thr but not Tyr phosphorylation was almost completely abolished in *mkk7*$^{-/-}$ cells (Fig. 4, *A* and *B*, *lanes 2–4*) in which stress-induced phosphorylation of SEK1 was retained at the same level as wild-type cells (Fig. 4, *D* and *E*, *lanes 5* and *6*). On the other hand, the Tyr phosphorylation of SAPK/JNK was greatly impaired in *sek1*$^{-/-}$ cells (Fig. 4*B*, *lanes 6–8*) in accordance with our previous report (10). Surprisingly, the Thr phosphorylation was also markedly attenuated in *sek1*$^{-/-}$ cells (Fig. 4*A*, *lanes 6–8*), although this mutant contained the same amount of 48-kDa MKK7 as wild-type cells (Fig. 1*D*). These results indicate that SEK1 phosphorylates the Tyr residue of SAPK/JNK and that MKK7 preferentially phosphorylates the Thr residue of Tyr-phosphorylated SAPK/JNK rather than its non-phosphorylated form. In other words, MKK7-induced Thr phosphorylation requires the prior phosphorylation of SAPK/JNK at the Tyr residue by SEK1 in the stress-stimulated ES cells (see Fig. 8*C*).

Loss of Stress-induced Thr Phosphorylation of SAPK/JNK in Cells Expressing a Kinase-dead Mutant of SEK1—In ES cells, SEK1 and MKK7 clearly contributed to the dual phosphorylation of SAPK/JNK in response to stress stimuli, and the MKK7-induced Thr phosphorylation seemed to require the prior Tyr phosphorylation by SEK1. Therefore, we further investigated the action of SEK1, which was supposed to be involved in the prior Tyr phosphorylation of SAPK/JNK. For the analysis, we used a human embryonic kidney cell line (293T) for transient transfection because of low efficiency of transfection into ES cells. HA-tagged JNK1 was co-expressed with FLAG-dnSEK1, which lacks kinase activity, in the cells using pCMV5 mammalian vectors. In a series of the experiments, the expression of HA-JNK1 was almost constant (Fig. 5*C*). Thr and Tyr phosphorylation of exogenous HA-JNK1 in response to 1 kJ/m^2 of UV irradiation was measured. UV irradiation induced the Thr and Tyr phosphorylation of HA-JNK1 (Fig. 5, *A* and *B*, *lane 3*); however, not only Tyr but also Thr phosphorylation was lost in the dnSEK1-expressing cells (Fig. 5, *A* and *B*, *lane 4*). These results clearly show that the stress-induced Thr phosphorylation of SAPK/JNK requires the prior Tyr phosphorylation by SEK1 in living cells.

Loss of Stress-induced Thr Phosphorylation of SAPK/JNK in Cells Expressing the No Tyr-phosphorylated Forms of SAPK/JNK—Next, we investigated the contribution of the Tyr residue in the Thr-Pro-Tyr motif of SAPK/JNK, phosphorylation of which was supposed to proceed before the Thr modification by MKK7 in the sequential phosphorylation. For the analysis, we constructed three kinds of HA-JNK1 mutants (APF, APY, and TPF), in which the Thr (T)-Pro (P)-Tyr (Y) motif was replaced with Ala (A), and Phe (F), respectively. The HA-JNK mutants and wild type were expressed in 293T cells by transfection, and the phosphorylation and kinase activity were measured. In a series of the experiments, the expression of HA-JNK1 was almost constant (Fig. 6*C*). The UV-induced Thr and Tyr phosphorylation and its ability to phosphorylate glutathione *S*-transferase-c-Jun as substrate could be detected in the wild-type HA-JNK1/TPY (Fig. 6, *lane 1*). Tyr phosphorylation of the HA-JNK/APY mutant was also detected (Fig. 6*B*, *lane 3*), although its kinase activity was completely lost (Fig. 6*D*, *lane 3*). Interestingly, the Thr phosphorylation could not be detected in the HA-JNK1/TPF mutant, in which the Tyr residue was re-

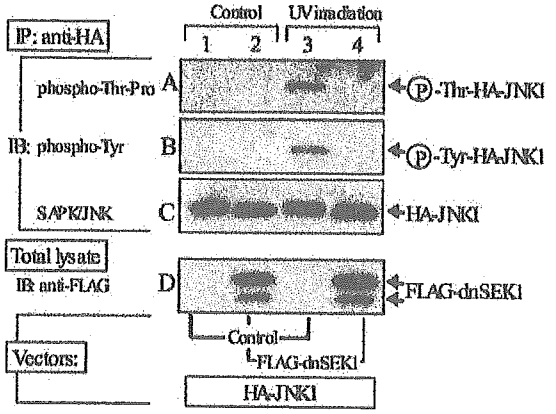

FIG. 5. **Effects of SEK1 inhibition on stress-induced Thr and Tyr phosphorylation of SAPK/JNK in 293T cells.** 293T cells were transfected with 1 μg of pCMV5/HA-JNK1, together with (*lanes 2* and *4*) or without (*lanes 1* and *3*) 1 μg of pCMV5/FLAG-dnSEK1. The transfected 293T cells, after being cultured for 24 h, were stimulated with 1 kJ/m^2 of UV irradiation and incubated for 25 min (*lanes 3* and *4*). Cell lysates were prepared, and HA-JNK1 was immunoprecipitated (*IP*) with anti-HA affinity matrix. The Thr phosphorylation (*A*) and Tyr phosphorylation (*B*) of HA-JNK1 were determined using anti-phospho Abs. HA-JNK1 (*C*) and FLAG-dnSEK1 (*D*) were determined using anti-SAPK/JNK (FL) and anti-FLAG (M2) Abs, respectively. *IB*, immunoblots.

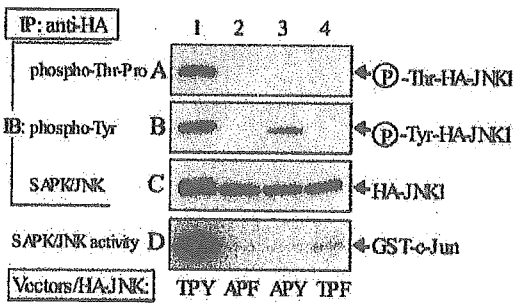

FIG. 6. **Effects of amino acid replacement of the TPY motif on the stress-induced Thr and Tyr phosphorylation of SAPK/JNK in 293T cells.** 293T cells were transfected with 1 μg of TPY-wild type (*lane 1*), APF- (*lane 2*), APY- (*lane 3*), and TPF- (*lane 4*) mutant forms of HA-JNK1 expression vectors. The transfected 293T cells, after being cultured for 24 h, were stimulated with 1 kJ/m^2 of UV irradiation and further incubated for 25 min. Cell lysates were prepared and immunoprecipitated (*IP*) with anti-HA affinity matrix. The Thr phosphorylation (*A*) and Tyr phosphorylation (*B*) of HA-JNK1 were determined using anti-phospho Abs. HA-JNK1 (*C*) was determined using anti-SAPK/JNK (FL) polyclonal Abs. The SAPK/JNK activity (*D*) was measured as described under "Experimental Procedures." *IB*, immunoblots.

placed by Phe (Fig. 6*A*, *lane 4*). These results clearly show that the stress-induced Thr phosphorylation of SAPK/JNK requires the phosphorylated Tyr residue in living cells.

SAPK/JNK Interacts More Preferentially with SEK1 than with MKK7—To understand the molecular mechanism of the prior Tyr phosphorylation of SAPK/JNK by SEK1, we examined the association of SAPK/JNK with SEK1. HA-JNK1 was co-expressed with FLAG-SEK1 and FLAG-MKK7γ2 in 293T cells using pCMV5 mammalian vectors (10). The transfected cells were stimulated with the protein synthesis inhibitor anisomycin. The cell lysates were immunoprecipitated with anti-HA affinity matrix and analyzed for the phosphorylation of SEK1 using anti-phospho-SEK1 and anti-FLAG Abs. The expression of HA-JNK1 was almost constant (Fig. 7*C*). The different ratios of FLAG-SEK1 and FLAG-MKK7γ2 expression vectors induced varied expression levels of FLAG-SEK1 and

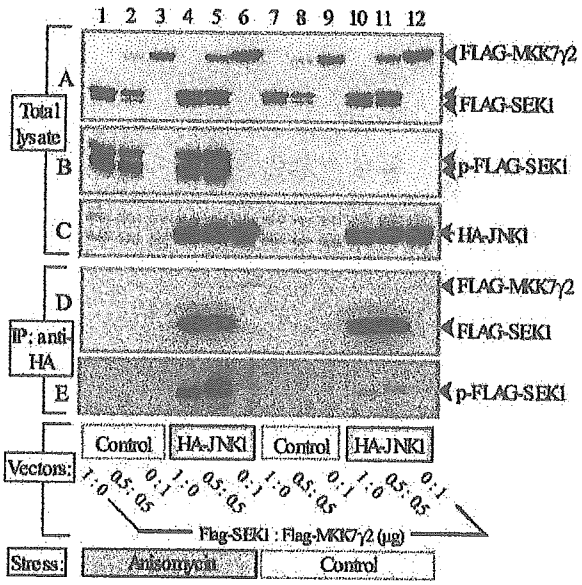

FIG. 7. **Preferential association of SAPK/JNK with SEK1.** 293T cells were transfected with different amounts (0, 0.5, or 1 μg) of pCMV5/FLAG-tagged SEK1 and/or MKK7γ2 expression vectors, together with (*lanes 4–6* and *10–12*) or without (*lanes 1–3* and *7–9*) 1 μg of pCMV5/HA-JNK1. The transfected 293T cells, after being cultured for 24 h, were stimulated with 3 μg/ml of anisomycin (*lanes 1–6*) or not (*lanes 7–12*). Cell lysates were prepared (*A–C*) and immunoprecipitated (*IP*) with anti-HA affinity matrix (*D* and *E*). Expression of SEK1 *plus* MKK7γ2 (*A*), phosphorylated SEK1 (*B*), and HA-JNK1 (*C*) were determined using anti-FLAG (M2), anti-phospho-SEK1, and anti-SAPK/JNK (FL) Abs, respectively. Co-immunoprecipitated SEK1 *plus* MKK7γ2 (*D*) and phosphorylated SEK1 (*E*) were determined using anti-FLAG (M2) and anti-phospho-SEK1, respectively.

FLAG-MKK7γ2 proteins, but the sum of the expressed proteins was almost constant in each of the experiments (Fig. 7*A*). FLAG-SEK1 was phosphorylated in response to anisomycin in the presence and absence of HA-JNK1 (Fig. 7*B*). Interestingly, both phosphorylated and non-phosphorylated forms of FLAG-SEK1 could be coimmunoprecipitated with HA-JNK1; however, FLAG-MKK7γ2 was not (Fig. 7, *D* and *E*). The interaction between SEK1 and SAPK/JNK seemed to be comparable with that observed between JIP-1 and SAPK/JNK (data not shown). These results clearly show that SAPK/JNK interacts more preferentially with SEK1 than with MKK7 and suggest that the interaction might be responsible for the prior Tyr phosphorylation of SAPK/JNK by SEK1 (see Fig. 8*C*).

We also examined whether the above interaction is observable in ES cells that did not overexpress the HA-JNK1 and FLAG-SEK1/MKK7γ2. However, we could not detect their direct interaction in the native ES cells or in mouse tissues, including brain and liver (data not shown). This may be because of low expression levels of the endogenous proteins. Alternatively, endogenous SEK1 may localize near or exist as a non-associated form with SAPK/JNK in native cells, and there may be a molecular mechanism for releasing SEK1 rapidly after the phosphorylation of SAPK/JNK.

DISCUSSION

It has been reported in *in vitro* experiments that synergistic activation of SAPK/JNK requires the phosphorylation of both Thr and Tyr residues within the Thr-Pro-Tyr motif by the two different activators, SEK1 and MKK7 (7–9). Although the two MAPKKs are capable of catalyzing both phosphorylations, SEK1 prefers the Tyr phosphorylation and MKK7 prefers the Thr phosphorylation *in vitro* (Fig. 8*A*). In a previous study, we

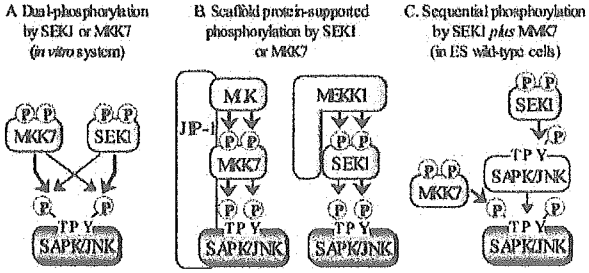

FIG. 8. **Schematic description of SAPK/JNK phosphorylation by SEK1 and MKK7 under various conditions.** *A*, synergistic activation of SAPK/JNK by the dual specificity kinase SEK1 or MKK7, which has been reported in *in vitro* conditions (7–9). *B*, activation of SAPK/JNK by SEK1 or MKK7 associated with their scaffold proteins, JIP-1 and MEKK1 (1, 2). *C*, synergistic activation of SAPK/JNK through sequential phosphorylation by SEK1 plus MKK7 in murine ES cells observed in the present study. See "Discussion" for further explanation. *TPY*, Thr-Pro-Tyr motif.

reported that SEK1 is essentially required for synergistic activation of SAPK/JNK in murine ES cells because the activation by various stresses was markedly attenuated in *sek1*$^{-/-}$ murine ES cells (10). This attenuation was accompanied with a decreased level of the Tyr phosphorylation. In the present study, we also generated *mkk7*$^{-/-}$ ES cells and compared the two mutant ES cells in terms of the activation and phosphorylation of SAPK/JNK. Our present results not only confirm the synergistic activation of SAPK/JNK reported previously but also indicate the unique properties of SEK1 and MKK7 in the stress-induced phosphorylation of the MAPK as follows.

First, MKK7 seemed to be a selective MAPKK for the synergistic activation and the Thr phosphorylation of SAPK/JNK. The mutant *mkk7*$^{-/-}$ ES cells had a defect in synergistic SAPK/JNK activation in response to a variety of stimuli (Fig. 2). This defect could be selectively rescued by the introduction of MKK7 isoforms (α1 and γ1) but not by SEK1 (Fig. 3*B*). Thr phosphorylation of SAPK/JNK observed in wild-type cells was almost completely abolished in *mkk7*$^{-/-}$ ES cells (Fig. 4*A*, *lanes 2–4*; see also Fig. 8*C*). Second, the properties of MKK7, which preferentially catalyzes Thr phosphorylation of SAPK/JNK, seemed to be dependent on another MAPKK, SEK1, because the Thr phosphorylation was greatly impaired in *sek1*$^{-/-}$ ES cells, which retain MKK7 expression (Fig. 4*A*, *lanes 6–8*). This idea was supported by the additional results as follows. 1) Inhibition of SEK1 by the expression of its dominant-negative form (dnSEK1) blocked Thr phosphorylation of SAPK/JNK in addition to Tyr modification. 2) The SAPK/JNK mutant (TPF), which lacks phosphorylatable Tyr residue, could not be phosphorylated at the Thr residue. 3) SEK1 could associate SAPK/JNK more preferentially than MKK7 and make a complex of SEK1 and SAPK/JNK without MKK7. Thus, we present a novel activation mechanism that SEK1-induced Tyr phosphorylation of SAPK/JNK is followed by additional Thr phosphorylation by MKK7 in stress-stimulated ES cells (Fig. 8*C*). In other words, MKK7 preferentially phosphorylates the Thr of Tyr-phosphorylated SAPK/JNK. On the other hand, SEK1 catalyzes Tyr phosphorylation of the MAPK in a manner independent on MKK7-induced Thr phosphorylation.

Tournier *et al.* have recently reported that the two MAPKKs, MKK7 and SEK1, differently contribute in various stress-induced activation of SAPK/JNK using primary murine embryo fibroblasts isolated from *sek1*$^{-/-}$, *mkk7*$^{-/-}$, and dual deficient mice (14). Their report shows that MKK7 is more important than SEK1 in the activation of SAPK/JNK by proinflammatory cytokines in murine embryo fibroblasts. SAPK/JNK activation in response to UV and anisomycin was almost completely lost in *sek1*$^{-/-}$ *mkk7*$^{-/-}$ murine embryo fibroblasts, but approximately half stimulation of SAPK/JNK was retained in *sek1*$^{-/-}$or *mkk7*$^{-/-}$ murine embryo fibroblasts. In contrast, SAPK/JNK activation in response to TNFα and IL-1α was almost completely lost in *mkk7*$^{-/-}$ cells, but 50% stimulation was observed in *sek1*$^{-/-}$ cells. Thus, their results are somewhat different from ours observed in the single mutant of *sek1*$^{-/-}$or *mkk7*$^{-/-}$ ES cells, where SAPK/JNK activation by various stimuli was greatly reduced. These differences may be caused by the specificity of cell types used. ES cells were derived directly from preimplantation embryos and maintained *in vitro* under undifferentiated conditions. Thus, the molecular mechanism of SAPK/JNK activation observable in ES cells may be considered a prototype in mammalian cells. In more differentiated cells, other cellular proteins, such as the JIP group of scaffold proteins, may regulate the protein interaction among SEK1, MKK7, and SAPK/JNK to alter the properties of the MAPKKs, resulting in the gain of dual-specificity kinase activity (Fig. 8*B*). However, overexpression of JIP1, -2, or -3 by cDNA transfection did not support this possibility (data not shown). Therefore, it will be critical to investigate the two phosphorylated states of the Thr-Pro-Tyr motif in endogenous SAPK/JNK and associated proteins to understand the molecular mechanism of synergistic activation of the MAPK in each type of cells.

Besides SAPK/JNK, other members of MAPK family, ERK and p38, have also two MAPKKs. ERK is activated by MKK1 and MKK2, and p38 is stimulated by MKK3 and MKK6 (15). Therefore, the presence of two MAPKKs is a common feature of mammalian MAPK-signaling pathways. Fleming *et al.* have reported that MKK3 and MKK6 have a strong preference for the phosphorylation of Tyr residue within the Thr-Gly-Tyr motif of p38 MAPK (9). Other MAPKKs have also unique biochemical properties. Therefore, ERK and p38 may be regulated cooperatively by two MAPKKs, as has been observed in SAPK/JNK. Studies in other MAPKK-deficient cells would be required for the elucidation of the functional significances of two activators in ERK and p38 MAPK-signaling pathways.

Recently, Ferrell *et al.* have proposed the interesting concept that SAPK/JNK cascade could, in principle, function as a sensitivity amplifier, which converts graded inputs into more switch-like outputs, allowing the cascade to filter out noise and yet still respond decisively to supra-threshold stimuli (16–19). They have shown in *Xenopus* oocytes that SAPK/JNK responds to physiological and pathological stimuli, such as progesterone and sorbitol, in an all-or-none manner (20). The activation of SAPK/JNK by the stimuli was graded at the level of a population of oocytes; however, at the level of an individual oocyte, the stimulatory response seemed to be switch-like. In the present study, we have also observed a very steep concentration-dependent response in the activation of SAPK/JNK by hyperosmolar stress (*i.e.* sorbitol) in murine ES cells (Fig. 2*E*). Furthermore, as described in the Introduction, our recent work showed that both SEK1 and MKK7 are required for full SAPK/JNK activation and hepatoblast proliferation in developing mice (6). This suggests that the all-or-none type MAPK activation also occurs in mammalian cells at an individual cell level only when the two MAPKKs are simultaneously activated. Therefore, this MAPK signaling should strictly proceed without errors, essentially through the two separated signals, one of which activates SEK1 and the other activates MKK7. Although the molecular mechanism whereby the two MAPKKs are simultaneously stimulated by various stress signals remains to be resolved, it is tempting to speculate that the existence of the two separated pathways leading to SAPK/JNK activation may

physiologically function as a fail-safe mechanism as proposed previously (10).

REFERENCES

1. Davis, R., J. (2000) *Cell* **103,** 239–252
2. Chang, L., and Karin, M. (2001) *Nature* **410,** 37–40
3. Yang, D., Tournier, C., Wysk, M., Lu, H.-T., Xu, J., and Davis, R. J. (1997) *Proc. Natl. Acad. Sci. U. S. A.* **94,** 3004–3009
4. Ganiatsas, S., Kwee, L., Fujiwara, Y., Perkins, A., Ikeda, T., Labow, M., A., and Zon, L. I. (1998) *Proc. Natl. Acad. Sci. U. S. A.* **95,** 6881–6886
5. Nishina, H., Vaz, C., Billia, P., Nghiem, M., Sasaki, T., Pompa, J. L., Furlonger, K., Paige, C., Hui, C.-C., Fischer, K. D., Kishimoto, H., Iwatsubo, T., Katada, T., Woodgett, J. R., and Penninger, J. M. (1999) *Development* **126,** 505–516
6. Watanabe, T., Nakagawa, K., Ohata, S., Kitagawa, D., Nishitai, G., Seo, J., Tanemura, S., Shimizu, N., Kishimoto, H., Wada, T., Aoki, J., Arai, H., Iwatsubo, T., Mochita, M., Watanabe, T., Satake, M., Ito, Y., Matsuyama, T., Mak, T. W., Penninger, J. M., Nishina, H., and Katada, T. (2002) *Dev. Biol.* **250,** 332–347
7. Lawler, S., Fleming, Y., Goedert, M., and Cohen, P. (1998) *Curr. Biol.* **8,** 1387–1390
8. Lisnock, J., Griffin, P., Calaycay, J., Franz, B., Parsons, J., O'Keefe, S. J., and LoGrasso, P. (2000) *Biochemistry* **39,** 3141–3148
9. Fleming, Y., Armstrong, C. G., Morrice, N., Paterson, A., Goedert, M., and Cohen, P. (2000) *Biochem. J.* **352,** 145–154
10. Wada, T., Nakagawa, K., Watanabe, T., Nishitai, G., Seo, J., Kishimoto, H., Kitagawa, D., Sasaki, T., Penninger, J. M., Nishina, H., and Katada, T. (2001) *J. Biol. Chem.* **276,** 30892–30897
11. Sasaki, T., Wada, T., Kishimoto, H., Irie-Sasaki, J., Matsumoto, G., Goto, T., Yao, Z., Wakeham, A., Mak, T. W., Suzuki, A., Katada, T., Nishina, H., and Penninger, J. M. (2001) *J. Exp. Med.* **194,** 757–768
12. Nishina, H., Fischer, K. D., Radvanyi, L., Shahinian, A., Hakem, R., Rubie, E. A., Bernstein, A., Mak, T. W., Woodgett, J. R., and Penninger, J. M. (1997) *Nature* **385,** 350–353
13. Nishina, H., Bachmann, M., Oliveira-dos-Santos, A. J., Kozieradzki, I., Fischer, K. D., Odermatt, B., Wakeham, A., Shahinian, A., Takimoto, H., Bernstein, A., Mak, T. W., Woodgett, J. R., Ohashi, P. S., and Penninger, J. M. (1997) *J. Exp. Med.* **186,** 941–953
14. Tournier, C., Dong, C., Turner, T. K., Jones, S. N., Flavell, R. A., and Davis, R. J. (2001) *Genes Dev.* **15,** 1419–1426
15. Schaeffer, H. J., and Weber, M. J. (1999) *Mol. Cell. Biol.* **19,** 2435–2444
16. Huang, C.-Y. F., and Ferrell, J. E., Jr. (1996) *Proc. Natl. Acad. Sci. U. S. A.* **93,** 10078–10083
17. Ferrell, J. E., Jr. (1996) *Trends Biochem. Sci.* **21,** 460–466
18. Ferrell, J. E., Jr. (1997) *Trends Biochem. Sci.* **22,** 288–289
19. Brown, G. C., Hoek, J. B., and Kholodenko, B. N. (1997) *Trends Biochem. Sci.* **22,** 288
20. Bagowski, C. P., and Ferrell, J. E., Jr. (2001) *Curr. Biol.* **11,** 1176–1182

Human Molecular Genetics, 2003, Vol. 12, No. 13 1535–1542
DOI: 10.1093/hmg/ddg168

Dentatorubral-pallidoluysian atrophy protein is phosphorylated by c-Jun NH_2-terminal kinase

Yuko Okamura-Oho[1], Toshiyuki Miyashita[1], Kazuaki Nagao[1], Seigo Shima[1], Yukie Ogata[1], Toshiaki Katada[2], Hiroshi Nishina[2] and Masao Yamada[1,*]

[1]Department of Genetics, National Research Institute for Child Health and Development, 3-35-31 Taishido, Setagaya-ku, Tokyo, 154-8567, Japan and [2]Department of Physiological Chemistry, Graduate School of Pharmaceutical Sciences, University of Tokyo, 7-3-1 Hongo, Bunkyo-ku, Tokyo, 113-0033, Japan

Received February 25, 2003; Revised and Accepted April 30, 2003

Dentatorubral-pallidoluysian atrophy (DRPLA) is a dominant-inherited neurodegenerative disease characterized by selective cell loss in particular neuronal pathways. This is caused by expansion of CAG repeats in the coding region of the DRPLA gene, and the extended polyglutamine tract (polyQ) confers a toxic activity. It is valuable to characterize disease gene products for elucidation of the mechanism underlying neuron death at specific anatomical areas of the brain. Here, we define the DRPLA protein as a phosphoprotein, and c-Jun NH_2-terminal kinase (JNK) is one of the major factors involved in its phosphorylation. Endogenous DRPLA protein was serine-phosphorylated. Phosphorylation was demonstrated in a recombinant JNK activation system *in vitro* and also in overexpressing cells by transfection after the JNK activation with osmotic pressure. One of the phospho-acceptor sites for JNK appearing in the DRPLA sequence was indeed phosphorylated, which was confirmed by a specific antibody raised against the phosphopeptide. Kinetic studies in the JNK recombinant system showed that expanded polyQ slightly reduced the affinity of JNK to the protein. Thus, the abnormal DRPLA protein seems to be slowly phosphorylated in a certain condition of JNK activation in patients. It may delay a process that is essential in keeping neurons alive.

INTRODUCTION

Dentatorubral-pallidoluysian atrophy (DRPLA) is a dominantly inherited neurodegenerative disease characterized by selective neuron loss in the cerebellar and pallidal outflow pathways (1). The disease is caused by expansion of CAG repeats in the coding region of the DRPLA gene, and the extended polyglutamine tract (polyQ) confers a toxic activity to a subset of neurons (2–4). Several other neurodegenerative diseases including Huntington disease are also known to be caused by expansion of CAG repeats in the coding region of the respective genes (5). Thus, these diseases are collectively called polyglutamine diseases. It has been demonstrated that over expression of extended polyQ induces apoptosis in a variety of cells (6,7), but the precise mechanism leading to apoptosis has not yet been settled. Previous studies have implied impairment of transcription, retardation in cleaning of misfolding proteins, sequestering of essential factors or formation of pores with extended polyQ (8–20). Although several studies have excluded the involvement of aggregates visible under a microscope in these processes (21–23), all the proposed mechanisms seem to imply the cohesive force of polyQ.

We have been studying the normal functions of the DRPLA product (24–27), also known as 'atrophin-1'. As a specific subset of neurons are degenerated in different polyglutamine diseases, polyQ alone is not enough to elucidate the pathogenesis of patients. We previously reported binding partners with DRPLA protein (25). Among them, IRSp53 and DVL1 potentially activate signaling cascades of c-Jun NH_2-terminal kinase (JNK), a family member of mitogen activated protein kinases (MAPKs), which phosphorylates serine/threonine (S/T) residues followed by proline (S/TP) (28–34). Seven other binding partners use phosphorylated S/T as a target (25,35). As there are many S/TP sequences in the DRPLA protein (4) (Fig. 1), we are interested on the phosphorylation state of the product. Recently, a DRPLA-like protein in Drosophila, Atro (or Grunge), was reported to have multiple functions in transcriptional regulation (36,37). It functions as a transcriptional co-repressor in the earliest stage of embryogenesis, and further participates in body patterning in multiple developmental stages as transcriptional regulators. Expression of the abnormal DRPLA protein with extended polyQ in Drosophila embryos causes deregulation of transcription. Atro/Grunge has

*To whom correspondence should be addressed. Tel: +81 334160181; Fax: +81 334122259; Email: myamada@nch.go.jp

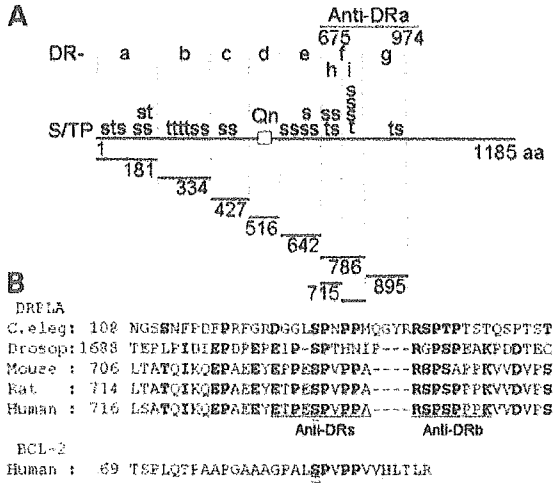

Figure 1. Putative phosphorylation sites in the DRPLA protein. (A) The amino acid sequence of the human DRPLA protein containing polyglutamine (Qn), serine (s) or threonine (t) followed by a proline residue (S/TP), fragments of the DRPLA protein (DR-a–i), and an antigen fragment used for generating the anti-human DRPLA antibody (anti-DRa) are indicated. (B) Conserved amino acid residues in the DR-i fragment of the human DRPLA protein and in the homologous portion of other species. Accession numbers of the genes are AF068719, NM_079249, XM_132846, NM_017228 and D31840. Conserved residues at least in four species are bold. Serine 734 in the DRPLA protein and serine 98 in human BCL-2 are double-underlined. Amino acid residues for generating an anti-DRPLA phospho-serine 734 antibody (anti-DRs) and an anti-DRPLA peptide antibody (anti-DRb) are underlined.

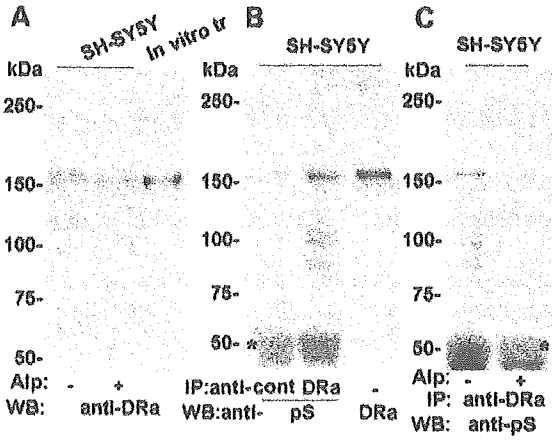

Figure 2. Phosphorylation of the DRPLA protein in cultured cells. (A) Treatment with alkaline phosphatase increases the mobility of the DRPLA protein through SDS–PAGE. Aliquots of neuroblastoma (SH-SY5Y) cell lysate were incubated with or without alkaline phosphatase (Alp + and –), applied to SDS–PAGE and blotted with an anti-recombinant DRPLA antibody (anti-DRa). The in vitro translation product of the DRPLA protein was in the parallel run. (B) and (C) DRPLA protein is serine-phosphorylated. Aliquots of cell lysate were immunoprecipitated with the anti-DRa antibody or a pre-immune serum (anti-DRa or cont), and analyzed by western blotting with an anti-phosphoserine antibody (pS). The molecular size of the DRPLA protein is indicated in the parallel run of cell lysate blotted with the anti-DRa antibody. The immunoprecipitated protein was treated with or without the alkaline phosphatase (Alp + and – in panel C). Bands indicated by asterisks are the heavy chains of immunoglobulin.

evolved into two descendants, DRPLA and RERE, in mammals (4,26). Although human DRPLA protein lacks a putative DNA-binding domain in the N-terminal portion of the Drosophila homolog, it may be still be involved in transcriptional regulation as it gains additional motifs in the flanking region of polyQ. In light of these observations, we have characterized the phosphorylated state of the DRPLA protein and detected phosphorylation by JNK.

RESULTS

Endogenous DRPLA protein was phosphorylated

We first examined a phosphorylated state of the DRPLA protein in cultured cells (Fig. 2). The major form of the DRPLA protein in human neuroblastoma cells moved to the position of a 160 kDa protein through SDS–PAGE and was visualized with anti-human DRPLA antibody (anti-DRa), as shown previously (24). When the cell lysate was treated with alkaline phosphatase, the major form moved faster through SDS–PAGE and migrated to the same position as the in vitro translated product without post-translational modification (Fig. 2A). The major form precipitated with the anti-DRa antibody from the cell lysate was immuno-reactive to an anti-phosphoserine antibody (anti-pS), and it almost lost the reactivity when treated with the alkaline phosphatase (Fig. 2B and C). These results indicated that the major form of DRPLA protein in cultured cells was serine-phosphorylated.

DRPLA protein was phosphorylated by JNK in vitro

In an attempt to establish a biochemical basis for the phosphorylation, we adopted an in vitro activation system for JNK in which purified forms of recombinant protein kinases were mixed together. In this mixture, JNK3 is synergistically activated by two forms of MAPK kinase (MKK), constitutive active MKK7 and native MKK4 that is activated by constitutive active MEK kinase 1 (MEKK1), as described previously (38–40).

In vitro translation products of DRPLA with normal or expanded repeats were subjected to the activation system and analyzed by SDS–PAGE. When incubated in the JNK mixture, the translation products migrated more slowly than the untreated counterparts (Fig. 3A, upper panel). As the mobility shift was not observed by omission of any member of the four kinases from the reaction, the shift must be due to synergistically activated JNK as previously demonstrated. The products translated in unlabeled conditions, were radiolabeled after incubation in the mixture containing [γ-^{32}P]ATP (Fig. 3A, lower panel). When JNK-reacted products were further treated with alkaline phosphatase, the products moved faster than the untreated counterparts (Fig. 3B). Thus, we concluded that the normal and abnormal forms of the DRPLA protein were phosphorylated by JNK in vitro.

A time course study of phosphorylation showed that both the normal and abnormal DRPLA proteins were fully phosphorylated within 120 min (Fig. 3C and D). However, a

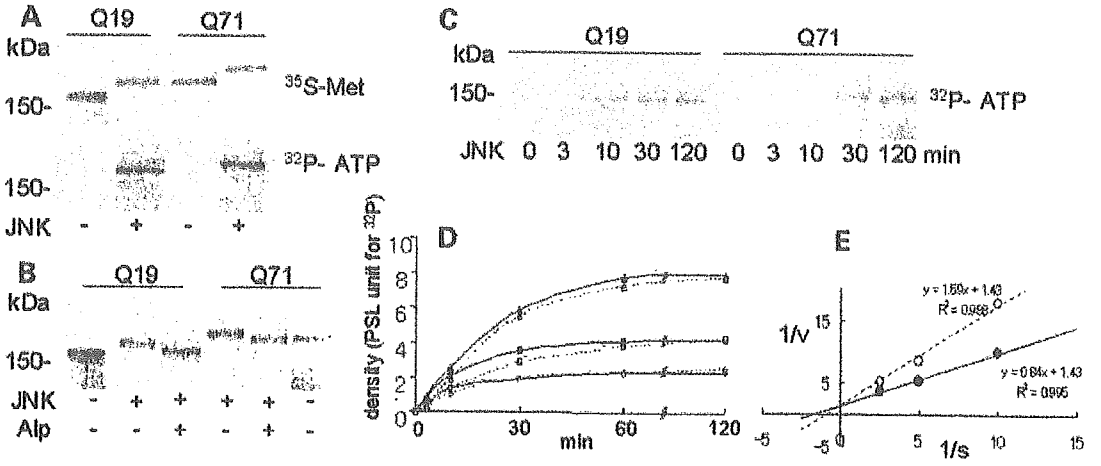

Figure 3. Phosphorylation of the full-length DRPLA protein in the recombinant activation system for JNK. In vitro translation products of the full-length DRPLA protein containing normal (Q19) and abnormal (Q71) polyQ were incubated in the recombinant JNK mixture. (A) The DRPLA protein labeled with [^{35}S]methionine (^{35}S-Met) was treated with or without the JNK reaction mixture (+ or −) for 1 h and applied on SDS–PAGE (upper panel). Non-labeled DRPLA protein was incubated in the mixtures containing [γ-^{32}P]ATP for 1 h and the phosphorylation was detected by autoradiography (lower panel). (B) The DRPLA protein labeled with [^{35}S]methionine was treated with or without alkaline phosphatase (Alp + or −), and resolved through SDS–PAGE with parallel run of products incubated in an incomplete JNK reaction mixture (JNK−). The indicated lanes were the results after omission of recombinant JNK, omission of any member of four kinases from the reaction abolished the mobility shift as well as incorporation of [γ-^{32}P]ATP. (C–E) Kinetic analysis of phosphorylation of the DRPLA protein by JNK. In vitro translation products (diamond, 1 U; square, 2 U; and triangle, 4 U) of the normal (Q19, solid symbols) and abnormal (Q71, open symbols) DRPLA proteins were incubated in 10 µl of the JNK mixture containing [γ-^{32}P]ATP for the indicated periods, and subjected to SDS–PAGE. A representative result of the autoradiographs in duplicates of three independent experiments is shown in (C). The extent of phosphorylation was quantified with radioactivity in the target proteins and plotted along incubation periods (D). The initial velocity (v) was calculated in the substrate content (s), and the double reciprocal plot (1/v versus 1/s) was used for evaluation of K_m (E).

kinetic analysis showed that the affinity of JNK for the abnormal protein was lower than that of the normal protein ($K_m = 0.59$ U/µl for the normal protein and 1.11 U/µl for the abnormal protein in Fig. 3E). Thus, the expanded polyQ reduced the affinity of JNK for the DRPLA protein.

To further investigate the phospho-acceptor sites, we produced seven non-overlapping fragments of the DRPLA protein (DR-a–i, shown in Fig. 1A). When subjected to the recombinant system, one of the fragments, DR-f, was strongly phosphorylated in the mixture (Fig. 4). In the absence of recombinant JNK3, the phosphorylation was completely eliminated (lanes f and f* in Fig. 4; note that the band for JNK3 also disappeared in lane f*). This clearly showed that the DR-f fragment was directly phosphorylated by JNK3. When the fragment was separated into two portions (DR-h and -i in Fig. 1A), both were phosphorylated (Fig. 4, lanes h and i). Thus, DR-f was thought to contain at least two phospho-acceptor sites, one of which was located in DR-h and the other in DR-i. Although the details were not examined, two other fragments, DR-a and -g, seem to have additional minor phospho-acceptor sites (Fig. 4, lanes a and g).

Figure 4. Phosphorylation of fragments of the DRPLA protein in the recombinant activation system for JNK. Equivalent amounts of the fragments of the DRPLA protein (DR-a–i, illustrated in Fig. 1A) were produced as GST-fusion proteins and visualized in western blotting with an anti-GST antibody (lower panels). They were incubated in the mixture containing JNK3 (closed triangle in upper panels), MKK4 (open triangle), constitutive active forms of MKK7 and MEKK1, and [γ-^{32}P]ATP for 30 min. The phosphorylation is detected with the radioactivity of the fragments (upper panels). Recombinant JNK3 was omitted in the last lane (f*). GST and c-Jun were used as positive and negative control substrates. Experiments were repeated three times and representative results are shown.

DRPLA protein over-expressed in cells was phosphorylated by JNK

Endogenous DRPLA protein was phosphorylated as shown in Figure 2. Then, we tested the phosphorylated state of over expressed forms of the normal and abnormal protein, tagged with HA at the N-terminal end, in neuroblastoma cells (Fig. 5). We chose a high osmotic pressure by adding sorbitol to the cultured medium for transient activation of JNK. As demonstrated in Figure 5A, active JNK was increased to

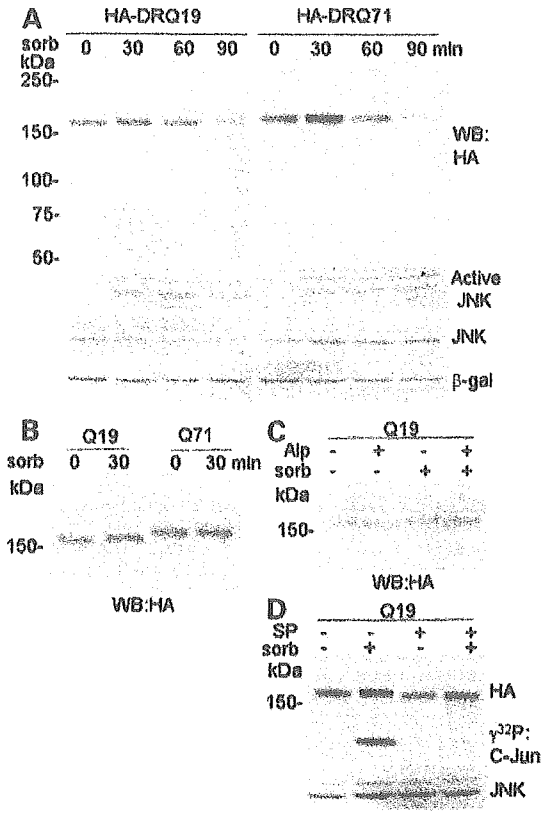

Figure 5. The overexpressed DRPLA protein is phosphorylated by JNK. Cells expressing HA-tagged normal and abnormal forms of the DRPLA protein (HA-DRQ19 and Q71) were incubated under a high osmotic condition with sorbitol for the indicated period (otherwise 30 min). The over-expressed protein was detected by western blotting with an anti-HA antibody (HA). The cell lysates were treated with alkaline phosphatase (Alp + in the panel C). The cells were incubated with the addition of JNK inhibitor, SP600125 (SP + in the panel D). The activity of JNK was monitored by western blotting with anti-active JNK antibody and by immune-complex kinase assay with c-Jun (A and D). The amount of total JNK and an unrelated protein (acid β-galactosidase) were monitored by western blotting with anti-JNK and β-galactosidase antibodies (D).

be detectable by western blotting with an anti-active JNK antibody. Along with the stimulation, amounts of the overexpressed forms of the DRPLA protein decreased afterward. It seemed that the N-terminal portion was cleaved off in the process, although the smaller fragments were not detected with the anti-HA antibody.

We examined the mobility shift of the normal DRPLA protein expressed in cells after osmotic stress. The mobility shift of the normal DRPLA was clear after 30 min of the stimulation (Fig. 5B), although the extent of the mobility shift shown here was less than that shown in the recombinant system (Q19 in Fig. 3A). The mobility shift of the abnormal protein was imperceptible. After the treatment of cell lysates with alkaline phosphatase, the normal protein with the osmotic stress migrated to the basal position without stress (Fig. 5C). Thus, the mobility shift was due to the phosphorylation state. When the cells were treated with a selective inhibitor of JNK, SP600125 (41) in the osmotic stress condition, the JNK kinase activity was inhibited as expected, and the normal protein migrated to the same position as the cells without osmotic stress (Fig. 5D). These results showed that DRPLA protein overexpressed in cultured cells was phosphorylated by JNK.

Serine 734 of the DRPLA protein is a phospho-acceptor site by JNK

We focused on phosphorylation of serine 734 (S734) in the DR-i fragment of DRPLA protein (double-underlined in Fig. 1B), because the flanking sequence, PESP, exactly matched the consensus sequence of phosphorylation by MAPKs (33). Moreover, the following sequence to S734 (SPVPP) is also found in BCL-2 (Fig. 1B) and the serine residue in the BCL-2 sequence is phosphorylated by JNK (42). To determine if the S734 residue in the DRPLA protein is essential for phosphorylation with JNK, we constructed a mutant fragment, DR-i734A, in which S734 was substituted to alanine. In contrast to the normal counterpart, the mutant fragment was not phosphorylated in the recombinant activation system and the immune complex kinase assay for JNK (Fig. 6A and B).

To show immunological evidence for phosphorylation of S734, we produced two antibodies (epitopes of which are shown in Fig. 1B) and assessed their specific reactivity in ELISA assay (Fig. 6C). The raised anti-phosphoserine 734 antibody (anti-DRs) reacted with the phosphorylated DR-i fragment in the recombinant JNK system, but not with non-phosphorylated counterparts in western blotting. The anti-DRPLA peptide antibody (anti-DRb) reacted with both (Fig. 6D). These results were consistent with the recombinant JNK system described above, and the S734 residue was the main target by JNK.

Serine 734 is phosphorylated in the rat brain

The rat DRPLA protein has 93% homology to its human counterpart and is smaller by two amino acid residues (43). Since the peptide sequences used for raising the anti-phosphopeptide antibodies are exactly the same in both species (Fig. 1B), we analyzed the phosphorylated state of the rat DRPLA protein by western blotting with the raised antibodies (Fig. 7). The expression level of the DRPLA protein detected with the anti-DRb antibody was consistent with our previous results on the level of mRNA in northern blotting (4); where it was high in the brain and low in the pancreas and testis (Fig. 7A). The major form in the brain (150 kDa protein) was also reactive with the anti-DRs antibody, which indicated that S734 in the DRPLA protein in the rat brain tissues was phosphorylated (Fig. 7B). This form was also detected with the anti-DRa antibody (data not shown). When the brain samples were treated with alkaline phosphatase, the major form migrated faster and almost lost the immunoreactivity to the anti-DRs antibody (Fig. 7C). These data were consistent with phosphorylation at S734.

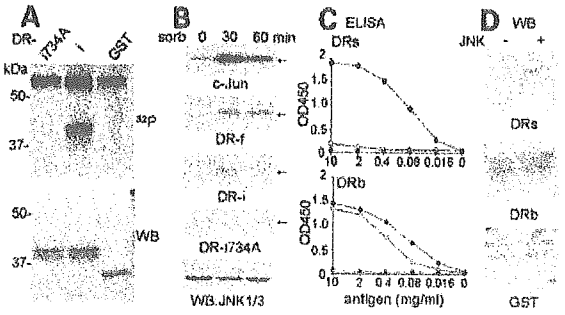

Figure 6. Serine 734 in the DRPLA protein is phosphorylated by JNK in vitro. (A) The fragment of DRPLA protein (DR-i), and its mutant form (DR-i734A, in which serine 734 was substituted to alanine) were subjected to the phosphorylation study with the recombinant activation system for JNK. (B) The indicated fragments of the DRPLA protein and c-Jun (with arrows) were used as a substrate for the immune-complex kinase assay of JNK. The neuroblastoma cells were treated with sorbitol for the indicated periods. Immunoprecipitated JNK was incubated with substrates and [γ-^{32}P]ATP. The phosphorylation of substrates was visualized by autoradiography. The amounts of precipitated JNK were monitored by western blotting (the last panel). (C) Specificity of two anti-peptide antibodies was tested by ELISA. Synthesized phosphorylated peptides (solid symbols), used for generating antibodies (DRs and DRb), and the non-phosphorylated counterparts (open symbols) were the antigen. Solid lines are for antibodies, and dotted lines for non-immune sera. (D) Anti-DRs antibody reacts with the fragment of DRPLA protein after phosphorylation by JNK. The fragment DR-i, treated with or without the recombinant JNK (+ or −), was blotted with anti-DRs, DRb and GST antibodies.

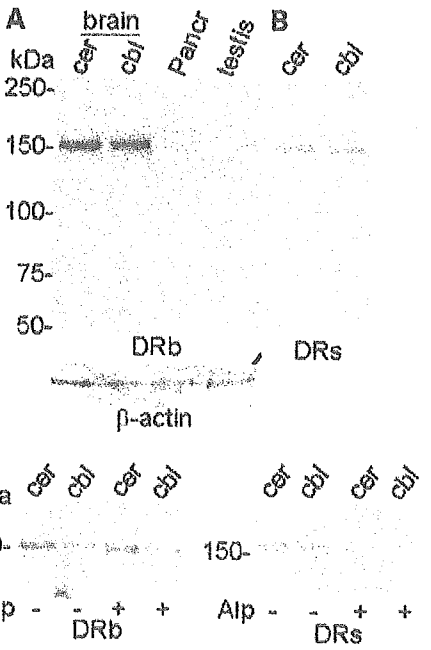

Figure 7. Serine 734 in the DRPLA protein in rat tissues is phosphorylated. (A–C) Western blotting of the DRPLA protein in rat tissues. Samples (30 μg of protein) obtained from the cerebrum (cer), cerebellum (cbl), pancreas (pancr) and testis were blotted with the anti-DRb, anti-DRs and anti-β actin antibodies. The brain samples in the parallel run were blotted with the anti-DRs in B. Samples were treated with or without alkaline phosphatase (Alp + or −) in (C).

DISCUSSION

We report evidence for phosphorylation of the DRPLA protein, the product of the gene responsible for the polyglutamine disease, dentatorubral-pallidoluysian atrophy. The endogenous form was phosphorylated and the phosphorylation was mainly mediated by JNK.

JNK is activated in the critical process of embryonic morphogenesis, as well as in response to environmental stress such as radiation and high osmotic pressure (44). The activation of JNK requires its phosphorylation mediated by MKK 4 and 7 (38,39). These two MKKs are activated by MKK kinases such as MEKK1. Activated JNK phosphorylates subsets of proteins including c-Jun, and up-regulates transcriptions of stress-responsive genes in various cells (45,46). In neurons, JNK3 is highly and consistently phosphorylated because of the synergistic activation of MKK4 and 7. Thus, DRPLA, one of the substrates of JNK3 as demonstrated in this report, may have a function in the brain coupled with activated JNK (47–49).

We identified the S734 residue of the DRPLA protein as a phospho-acceptor site in the recombinant system as well as in the brain tissues. However, phosphorylation of this residue was not detectable with the endogenous form of DRPLA protein in cultured cells with the same technique (data not shown). This may be accounted for by a weaker activity of JNK in cultured cells, while consistent activation of JNK is known in the brain at a similar level of the recombinant JNK system (49). The phosphorylation may be coupled to the activation of a protease. The molecular size of DRPLA protein detected in the rat brain with the specific phosphopeptide antibody was 150 kDa, which was slightly smaller than that expected from the sequence and the results with the human protein. The phosphorylated forms of HA-tagged human DRPLA gradually disappeared after osmotic treatment, as demonstrated in Fig. 5. Although we did not directly detect degraded forms, caspase-3 may be one of the candidates involved. We previously reported the DRPLA protein is a substrate of caspase-3 and about 10 kDa from the N-terminus was cleaved off (24).

Both the normal and abnormal forms of DRPLA protein were phosphorylated by the JNK recombinant system. However, precise kinetic analyses showed a reduced affinity of JNK for the abnormal protein. Furthermore, the abnormal protein expressed in cultured cells showed a subtle mobility shift in the JNK activation condition with osmotic pressure. It may be possible that a slight reduction of the affinity in the in vitro system causes considerable effects in a physiological condition, i.e. delay in a certain cascade reaction. Two other polyglutamine disease products, Huntingtin and androgen receptor, have recently been reported to be phosphorylated by an S/T kinase, Akt, which mediates the survival signal of IGF-I (50–52). As the DRPLA protein is already known to be situated in the insulin/IGF-I signaling cascade (25), three polyglutamine diseases products seem to be connected by the signal transduction of IGF-I. As IGF-I is one of the main neurotrophic factors, neurodegeneration in polyglutamine diseases may be solved by a function of IGF-I.

MATERIALS AND METHODS

Plasmid constructions

Original cDNA clones for DRPLA were previously described (2,4). The DNA fragment including the entire coding region of the DRPLA gene was subcloned into pBluescript SK(−) phagemid (Stratagene) for in vitro translation experiments, and a cpDNA-3xHA vector (kindly provided by Dr John C. Reed) for expression of HA-tagged proteins. cDNA fragments (shown in Fig. 1A) amplified by PCR methods were subcloned into a pGEX-3X vector (Pharmacia) to generate GST fusion proteins. Plasmid harboring a point mutation was obtained by PCR-mediated mutagenesis (53).

Antibodies

Epitopes for the following three antibodies are indicated in Figure 1. A rabbit polyclonal antibody which specifically reacted to a phosphorylated serine 734 residue in the DRPLA protein (anti-DRs) was raised against phosphopeptide ETPEpSPVPP (MBL Nagoya Japan). The serum was affinity-purified with the antigen peptide, and the reactivity to the non-phosphorylated peptide was eliminated with the affinity column. An anti-DRPLA peptide antibody (anti-DRb) was raised against phosphopeptide RSPpSPPPK, but it unexpectedly reacted to the non-phosphorylated counterpart as well as the antigen peptide. A rabbit polyclonal antibody raised against the recombinant human DRPLA protein (anti-DRa) was described previously (24). The following antibodies are also used: polyclonal anti-JNK1 antibody C-17 (Santa Cruz), monoclonal anti-JNK antibody (Pharmingen), anti-activated JNK antibody (Promega), monoclonal anti-phosphoserine antibody PSR-45 (Sigma), anti-HA antibody (Roche), anti-β actin antibody (Santa Crutz) and anti-human acid β-galactosidase antibody (54).

Preparation of recombinant proteins

Fragments of the DRPLA protein fused with GST were produced and purified as described previously (25). Translation products of the full-length DRPLA genes were produced with the TNT coupled reticulocyte lysate mixture in vitro (Promega). The radio-labeled and non-labeled products were made in the presence and absence of [^{35}S]methionine, respectively. To quantify the translation products, the labeled mixture was resolved by SDS–PAGE, and the radioactivity of the DRPLA protein was measured as Photo-Stimulated Luminescence (PSL) with a Fuji BAS 2000 PhosphorImager (Fuji Film, Japan). One unit (U) was defined as an amount of the mixture which gave 1 PSL unit/min of ^{35}S. The non-labeled mixtures, equivalent to 1, 2 and 4 U of the labeled counterparts, were subjected to the in vitro phosphorylation study.

In vitro phosphorylation assay in a recombinant activation system for JNK

In the recombinant system, JNK3 was synergistically activated by two forms of MKK, constitutive active MKK7 and native MKK4 that is activated by constitutive active MEKK1, as described previously (38–40). The mixture contains 100 ng of four GST-fusion proteins, JNK3, MKK4, MKK7 and MEKK1, in kinase buffer (50 mM Tris–Cl pH 7.5, 10 mM $MgCl_2$, 125 μM ATP, 1 mM DTT, 2 mM EDTA-Na and 500 μM $NaVO_4$). The fragments of the DRPLA protein fused with GST (100 ng equivalent) and the in vitro translation products of the DRPLA protein (1–4 U) were incubated in 10 μl of the mixture, with 5 μCi of [γ-^{32}P]ATP if needed, at 30°C for the indicated periods. Samples were resolved by SDS–PAGE and visualized with the PhosphorImager.

Cell culture

A human neuroblastoma cell line, SH-SY5Y, was maintained in RPMI1640 with 10% fetal bovine serum and transfected with plasmids using Lipofectamine PLUS (GIBCOBRL). For the activation of JNK with high osmotic pressure, cells were pre-incubated in the medium with 500 μM of Na_3VO_4 for 15 min. Then D(−)-sorbitol was added at a final concentration of 1 M and the incubation was continued for the indicated periods. For inhibition of the JNK kinase activity, a reversible ATP-competitive inhibitor, SP600125 (25 μM, BIOMOL), was added to the media 15 min prior to the sorbitol stimulation (41).

Immune complex protein kinase assay

SH-SY5Y cells were lysed in a lysis buffer (20 mM Tris–Cl pH 7.5, 150 mM NaCl, 1 mM EDTA, 1 mM EGTA, 1% Triton X-100, 2.5 mM sodium pyrophosphate, 1 mM β-glycerolphosphate, 1 mM Na_3VO_4, 1 μg/ml leupeptin and 1 mM PMSF). The lysates were sonicated and centrifuged. An aliquot of cleared lysates (100 μg of protein) was immunoprecipitated with the anti-JNK antibody C-17 for 2 h. The immune complex was used for a kinase assay with 5 μCi of [γ-^{32}P]ATP and 2 μg of the GST-fusion protein in a kinase buffer (20 mM Hepes pH 7.4, 10 mM $MgCl_2$ and 200 μM Na_3VO_4). After incubation at 30°C for 30 min, the samples were resolved by SDS–PAGE. One-tenth of the immune complex was analyzed by western blotting with an anti-monoclonal anti-JNK antibody.

Phosphatase treatment

SH-SY5Y cells and tissues from adult rats (male, Wistar rats) were homogenized in the Tris/$MgCl_2$ buffer (50 mM Tris-Cl pH 7.5 and 1 mM $MgCl_2$), sonicated for 30 s and centrifuged. Cleared lysates were incubated with calf intestine alkaline phosphatase (2 U for 10 μg protein, Sigma) at 30°C for 15 min, and the reaction was terminated with phosphatase inhibitors (Sigma).

Western blotting, immunoprecipitation and ELISA assay

The details of procedures for immunoprecipitation and western blotting were described previously (25). Briefly, an aliquot containing 100 ng of GST-fusion proteins, and 30 μg of protein extracts was subjected to western blotting with 1:500, 1:500, 1:200, 1:200 and 1:1000 diluted anti-GST, DRa, DRb, DRs and HA antibodies, respectively. To confirm equal loading of protein samples, the blotted membranes were re-probed with

the 1:400 and 1:250 diluted anti-β actin and anti-β galactosidase antibodies, respectively. The endogenous DRPLA protein was immunoprecipitated with the anti-DRa antibody from 500 μg protein of cell lysates and blotted with the 1:100 diluted anti-phosphoserine antibody. The ELISA assay using synthetic peptides as antigens and titration assays with anti-DRb and anti-DRs antibodies were performed according to the standard methods.

ACKNOWLEDGEMENTS

We wish to acknowledge Professor Yoshiyuki Suzuki (International University of Health and Welfare) for important suggestions and critical reading of the manuscript. We also thank A. Asaka and Y. Ohtsuka for technical assistance and K. Saito for preparing the manuscript. This study was supported in part by Grants for Human Genome, Brain Science and Pediatric Research from the Ministry of Health, Labor and Welfare, and a Grant for Organized Research Combination System from the Ministry of Education, Culture, Sports, Science and Technology, Japan.

REFERENCES

1. Naito, H. and Oyanagi, S. (1982) Familial myoclonus epilepsy and choreoathetosis: hereditary dentatorubral-pallidoluysian atrophy. Neurology, 32, 798–807.
2. Nagafuchi, S., Yanagisawa, H., Sato, K., Shirayama, T., Ohsaki, E., Bundo, M., Takeda, T., Tadokoro, K., Kondo, I., Murayama, N. et al. (1994) Dentatorubral and pallidoluysian atrophy expansion of an unstable CAG trinucleotide on chromosome 12p. Nat. Genet., 6, 14–18.
3. Koide, R., Ikeuchi, T., Onodera, O., Tanaka, H., Igarashi, S., Endo, K., Takahashi, H., Kondo, R., Ishikawa, A., Hayashi, T. et al. (1994) Unstable expansion of CAG repeat in hereditary dentatorubral-pallidoluysian atrophy (DRPLA). Nat. Genet., 6, 9–13.
4. Nagafuchi, S., Yanagisawa, H., Ohsaki, E., Shirayama, T., Tadokoro, K., Inoue, T. and Yamada, M. (1994) Structure and expression of the gene responsible for the triplet repeat disorder, dentatorubral and pallidoluysian atrophy (DRPLA). Nat. Genet., 8, 177–182.
5. Zoghbi, H.Y. and Orr, H.T. (2000) Glutamine repeats and neurodegeneration. A. Rev. Neurosci., 23, 217–247.
6. Ikeda, H., Yamaguchi, M., Sugai, S., Aze, Y., Narumiya, S. and Kakizuka, A. (1996) Expanded polyglutamine in the Machado-Joseph disease protein induces cell death in vitro and in vivo. Nat. Genet., 13, 196–202.
7. Warrick, J.M., Paulson, H.L., Gray-Board, G.L., Bui, Q.T., Fischbeck, K.H., Pittman, R.N. and Bonini, N.M. (1998) Expanded polyglutamine protein forms nuclear inclusions and causes neural degeneration in Drosophila. Cell, 93, 939–949.
8. Orr, H.T. (2001) Beyond the Qs in the polyglutamine diseases. Genes Dev., 15, 925–932.
9. Monoi, H. (1995) New tubular single-stranded helix of poly-L-amino acids suggested by molecular mechanics calculations: I. Homopolypeptides in isolated environments. Biophys. J., 69, 1130–1141.
10. Miyashita, T., Nagao, K., Ohmi, K., Yanagisawa, H., Okamura-Oho, Y. and Yamada, M. (1998) Intracellular aggregate formation of dentatorubral-pallidoluysian atrophy (DRPLA) protein with the extended polyglutamine. Biochem. Biophys. Res. Commun., 249, 96–102.
11. Shimohata, T., Nakajima, T., Yamada, M., Uchida, C., Onodera, O., Naruse, S., Kimura, T., Koide, R., Nozaki, K., Sano, Y. et al. (2000) Expanded polyglutamine stretches interact with TAFII130, interfering with CREB-dependent transcription. Nat. Genet., 26, 29–36.
12. McCampbell, A., Taylor, J.P., Taye, A.A., Robitschek, J., Li, M., Walcott, J., Merry, D., Chai, Y., Paulson, H., Sobue, G. et al. (2000) CREB-binding protein sequestration by expanded polyglutamine. Hum. Mol. Genet., 9, 2197–2202.
13. Nucifora, F.C.J., Sasaki, M., Peters, M.F., Huang, H., Cooper, J.K., Yamada, M., Takahashi, H., Tsuji, S., Troncoso, J., Dawson, V.L. et al. (2001) Interference by huntingtin and atrophin-1 with cbp-mediated transcription leading to cellular toxicity. Science, 291, 2423–2428.
14. Bence, N.F., Sampat, R.M. and Kopito, R.R. (2001) Impairment of the ubiquitin-proteasome system by protein aggregation. Science, 292, 1552–1555.
15. Suhr, S.T., Senut, M.C., Whitelegge, J.P., Faull, K.F., Cuizon, D.B. and Gage, F.H. (2001) Identities of sequestered proteins in aggregates from cells with induced polyglutamine expression. J. Cell Biol., 153, 283–294.
16. Abel, A., Walcott, J., Woods, J., Duda, J. and Merry, D.E. (2001) Expression of expanded repeat androgen receptor produces neurologic disease in transgenic mice. Hum. Mol. Genet., 10, 107–116.
17. Cummings, C.J., Sun, Y., Opal, P., Antalffy, B., Mestril, R., Orr, H.T., Dillmann, W.H. and Zoghbi, H.Y. (2001) Over-expression of inducible HSP70 chaperone suppresses neuropathology and improves motor function in SCA1 mice. Hum. Mol. Genet., 10, 1511–1518.
18. Dorsman, J.C., Pepers, B., Langenberg, D., Kerkdijk, H., Ijszenga, M., den Dunnen, J.T., Roos, R.A. and van Ommen, G.J. (2002) Strong aggregation and increased toxicity of polyleucine over polyglutamine stretches in mammalian cells. Hum. Mol. Genet., 11, 1487–1496.
19. Ravikumar, B., Duden, R. and Rubinsztein, D.C. (2002) Aggregate-prone proteins with polyglutamine and polyalanine expansions are degraded by autophagy. Hum. Mol. Genet., 11, 1107–1117.
20. Jiang, H., Nucifora, F.C. Jr, Ross, C.A. and DeFranco, D.B. (2003) Cell death triggered by polyglutamine-expanded huntingtin in a neuronal cell line is associated with degradation of CREB-binding protein. Hum. Mol. Genet., 12, 1–12.
21. Klement, I.A., Skinner, P.J., Kaytor, M.D., Yi, H., Hersch, S.M., Clark, H.B., Zoghbi, H.Y. and Orr, H.T. (1998) Ataxin-1 nuclear localization and aggregation: role in polyglutamine-induced disease in SCA1 transgenic mice. Cell, 95, 41–53.
22. Saudou, F., Finkbeiner, S., Devys, D. and Greenberg, M.E. (1998) Huntingtin acts in the nucleus to induce apoptosis but death does not correlate with the formation of intranuclear inclusions. Cell, 95, 55–66.
23. Yu, Z.X., Li, S.H., Nguyen, H.P. and Li, X.J. (2002) Huntingtin inclusions do not deplete polyglutamine-containing transcription factors in HD mice. Hum. Mol. Genet., 11, 905–914.
24. Miyashita, T., Okamura-Oho, Y., Mito, Y., Nagafuchi, S. and Yamada, M. (1997) Dentatorubral pallidoluysian atrophy (DRPLA) protein is cleaved by caspase-3 during apoptosis. J. Biol. Chem., 272, 29238–29242.
25. Okamura-Oho, Y., Miyashita, T., Ohmi, K. and Yamada, M. (1999) Dentatorubral-pallidoluysian atrophy protein interacts through a proline-rich region near polyglutamine with the SH3 domain of an insulin receptor tyrosine kinase substrate. Hum. Mol. Genet., 8, 947–957.
26. Yanagisawa, H., Bundo, M., Miyashita, T., Okamura-Oho, Y., Tadokoro, K., Tokunaga, K. and Yamada, M. (2000) Protein binding of a DRPLA family through arginine-glutamic acid dipeptide repeats is enhanced by extended polyglutamine. Hum. Mol. Genet., 9, 1433–1442.
27. Okamura-Oho, Y., Miyashita, T. and Yamada, M. (2001) Distinctive tissue distribution and phosphorylation of IRSp53 isoforms. Biochem. Biophys. Res. Commun., 289, 957–960.
28. Coso, O.A., Chiariello, M., Yu, J.C., Teramoto, H., Crespo, P., Xu, N., Miki, T. and Gutkind, J.S. (1995) The small GTP-binding proteins Rac1 and Cdc42 regulate the activity of the JNK/SAPK signaling pathway. Cell, 81, 1137–1146.
29. Minden, A., Lin, A., Claret, F.X., Abo, A. and Karin, M. (1995) Selective activation of the JNK signaling cascade and c-Jun transcriptional activity by the small GTPases Rac and Cdc42Hs. Cell, 81, 1147–1157.
30. Miki, H., Yamaguchi, H., Suetsugu, S. and Takenawa, T. (2000) IRSp53 is an essential intermediate between Rac and WAVE in the regulation of membrane ruffling. Nature, 408, 732–735.
31. Axelrod, J.D., Miller, J.R., Shulman, J.M., Moon, R.T. and Perrimon, N. (1998) Differential recruitment of Dishevelled provides signaling specificity in the planar cell polarity and Wingless signaling pathways. Genes Dev., 12, 2610–2622.
32. Boutros, M., Paricio, N., Strutt, D.I. and Mlodzik, M. (1998) Dishevelled activates JNK and discriminates between JNK pathways in planar polarity and wingless signaling. Cell, 94, 109–118.
33. Clark-Lewis, I., Sanghera, J.S. and Pelech, S.L. (1991) Definition of a consensus sequence for peptide substrate recognition by p44mpk, the meiosis-activated myelin basic protein kinase. J. Biol. Chem., 266, 15180–15184.

34. Deng, T. and Karin, M. (1994) c-Fos transcriptional activity stimulated by H-Ras-activated protein kinase distinct from JNK and ERK. Nature, 371, 171–175.
35. Wood, J.D., Yuan, J., Margolis, R.L., Colomer, V., Duan, K., Kushi, J., Kaminsky, Z., Kleiderlein, J.J., Sharp, A.H. and Ross, C.A. (1998) Atrophin-1, the DRPLA gene product, interacts with two families of WW domain-containing proteins. Mol. Cell Neurosci., 11, 149–160.
36. Zhang, S., Xu, L., Lee, J. and Xu, T. (2002) Drosophila atrophin homolog functions as a transcriptional corepressor in multiple developmental processes. Cell, 108, 45–56.
37. Erkner, A., Roure, A., Charroux, B., Delaage, M., Holway, N., Core, N., Vola, C., Angelats, C., Pages, F., Fasano, L. et al. (2002) Grunge, related to human Atrophin-like proteins, has multiple functions in Drosophila development. Development, 129, 1119–1129.
38. Lawler, S., Fleming, Y., Goedert, M. and Cohen, P. (1998) Synergistic activation of SAPK1/JNK1 by two MAP kinase kinases in vitro. Curr. Biol., 8, 1387–1390.
39. Wada, T., Nakagawa, K., Watanabe, T., Nishitai, G., Kishimoto, H., Kitagawa, D., Sasaki, T., Penninger, J.M., Nishina, H. and Katada, T. (2001) Impaired synergistic activation of stress-activated protein kinase SAPK/JNK in mouse embryonic stem cells lacking SEK1/MKK4: different contribution of SEK2/MKK7 isoforms to the synergistic activation. J. Biol. Chem., 276, 30892–30897.
40. Sasaki, T., Wada, T., Kishimoto, H., Irie-Sasaki, J., Matsumoto, G., Goto, T., Yao, Z., Wakeham, A., Mak, T.W., Suzuki, A. et al. (2001) The stress kinase mitogen-activated protein kinase kinase (MKK)7 is a negative regulator of antigen receptor and growth factor receptor-induced proliferation in hematopoietic cells. J. Exp. Med., 194, 757–768.
41. Bennett, B.L., Sasaki, D.T., Murray, B.W., O'Leary, E.C., Sakata, S.T., Xu, W., Leisten, J.C., Motiwala, A., Pierce, S., Satoh, Y. et al. (2001) SP600125, an anthrapyrazolone inhibitor of Jun N-terminal kinase. Proc. Natl Acad. Sci. USA, 98, 13681–13686.
42. Yamamoto, K., Ichijo, H. and Korsmeyer, S.J. (1999) BCL-2 is phosphorylated and inactivated by an ASK1/Jun N-terminal protein kinase pathway normally activated at G(2)/M. Mol. Cell. Biol., 19, 8469–8478.
43. Loev, S.J., Margolis, R.L., Young, W.S., Li, S.H., Schilling, G., Ashworth, R.G. and Ross, C.A. (1995) Cloning and expression of the rat atrophin-I (DRPLA disease gene) homologue. Neurobiol. Dis., 2, 129–138.
44. Davis, R.J. (2000) Signal transduction by the JNK group of MAP kinases. Cell, 103, 239–252.
45. Pulverer, B.J., Kyriakis, J.M., Avruch, J., Nikolakaki, E. and Woodgett, J.R. (1991) Phosphorylation of c-jun mediated by MAP kinases. Nature, 353, 670–674.
46. Kyriakis, J.M., Banerjee, P., Nikolakaki, E., Dai, T., Rubie, E.A., Ahmad, M.F., Avruch, J. and Woodgett, J.R. (1994) The stress-activated protein kinase subfamily of c-Jun kinases. Nature, 369, 156–160.
47. Mohit, A.A., Martin, J.H. and Miller, C.A. (1995) p493F12 kinase: a novel MAP kinase expressed in a subset of neurons in the human nervous system. Neuron, 14, 67–78.
48. Yao, R., Yoshihara, M. and Osada, H. (1997) Specific activation of a c-Jun NH_2-terminal kinase isoform and induction of neurite outgrowth in PC-12 cells by staurosporine. J. Biol. Chem., 272, 18261–18266.
49. Coffey, E.T., Hongisto, V., Dickens, M., Davis, R.J. and Courtney, M.J. (2000) Dual roles for c-Jun N-terminal kinase in developmental and stress responses in cerebellar granule neurons. J. Neurosci., 20, 7602–7613.
50. Lin, H.K., Yeh, S., Kang, H.Y. and Chang, C. (2001) Akt suppresses androgen-induced apoptosis by phosphorylating and inhibiting androgen receptor. Proc. Natl Acad. Sci. USA, 98, 7200–7205.
51. Humbert, S., Bryson, E.A., Cordelieres, F.P., Connors, N.C., Datta, S.R., Finkbeiner, S., Greenberg, M.E. and Saudou, F. (2002) The IGF-1/Akt pathway is neuroprotective in Huntington's disease and involves Huntingtin phosphorylation by Akt. Dev. Cell, 2, 831–837.
52. Brunet, A., Datta, S.R. and Greenberg, M.E. (2001) Transcription-dependent and -independent control of neuronal survival by the PI3K-Akt signaling pathway. Curr. Opin. Neurobiol., 11, 297–305.
53. Imai, Y., Matsushima, Y., Sugimura, T. and Terada, M. (1991) A simple and rapid method for generating a deletion by PCR. Nucl. Acids Res., 19, 2785.
54. Okamura-Oho, Y., Zhang, S., Hilson, W., Hinek, A. and Callahan, J.W. (1996) Early proteolytic cleavage with loss of a C-terminal fragment underlies altered processing of the beta-galactosidase precursor in galactosialidosis. Biochem. J., 313, 787–794.

Available online at www.sciencedirect.com

SCIENCE DIRECT®

ELSEVIER

Biochemical and Biophysical Research Communications 313 (2004) 1110–1118

BBRC

www.elsevier.com/locate/ybbrc

A subpopulation of bone marrow cells depleted by a novel antibody, anti-Liv8, is useful for cell therapy to repair damaged liver☆,☆☆

Naoki Yamamoto,[a] Shuji Terai,[a,*,1] Shinya Ohata,[b] Tomomi Watanabe,[b] Kaoru Omori,[a] Koh Shinoda,[c] Koji Miyamoto,[d] Toshiaki Katada,[b] Isao Sakaida,[a] Hiroshi Nishina,[b] and Kiwamu Okita[a]

[a] *Department of Molecular Science and Applied Medicine (Gastroenterology and Hepatology), Yamaguchi University School of Medicine, Minami Kogushi 1-1-1, Ube, Yamaguchi 755-8505, Japan*

[b] *Department of Physiological Chemistry, Graduate School of Pharmaceutical Science, University of Tokyo, Hongo 7-3-1, Bunkyoku, Tokyo 113 0033, Japan*

[c] *Department of Neuro-anatomy and Neuroscience, Yamaguchi University School of Medicine, Minami Kogushi 1-1-1, Ube, Yamaguchi 755-8505, Japan*

[d] *Department of Molecular Science and Applied Medicine (Kampo Medicine), Yamaguchi University School of Medicine, Minami Kogushi 1-1-1, Ube, Yamaguchi 755-8505, Japan*

Received 2 December 2003

Abstract

We previously reported a new in vivo model named as "GFP/CCl_4 model" for monitoring the transdifferentiation of green fluorescent protein (GFP) positive bone marrow cell (BMC) into albumin-positive hepatocyte under the specific "niche" made by CCl_4 induced persistent liver damage, but the subpopulation which BMCs transdifferentiate into hepatocytes remains unknown. Here we developed a new monoclonal antibody, anti-Liv8, using mouse E 11.5 fetal liver as an antigen. Anti-Liv8 recognized both hematopoietic progenitor cells in fetal liver at E 11.5 and CD45-positive hematopoietic cells in adult bone marrow. We separated Liv8-positive and Liv8-negative cells and then transplanted these cells into a continuous liver damaged model. At 4 weeks after BMC transplantation, more efficient repopulation and transdifferentiation of BMC into hepatocytes were seen with Liv8-negative cells. These findings suggest that the subpopulation of Liv8-negative cells includes useful cells to perform cell therapy on repair damaged liver.

Keywords: Bone marrow cell; Cell therapy; Regenerative medicine; Hepatic stem cell; Migration; Transdifferentiation; Mesenchymal stem cell; Hematopoietic stem cell; Liver regeneration; Niche

Recently, several groups have reported the possible plasticity of bone marrow cells (BMCs) to transdifferentiate into a variety of non-hematopoietic cell lineages [1–4]. Ever since the transdifferentiation of BMC into hepatocytes was documented following a bone marrow transplant from a man donor to a woman recipient [5,6],

☆ *Abbreviations:* BMC, bone marrow cell; CCl_4, carbon tetrachloride; FAH, fumarylacetoacetate hydrolase; GFP, green fluorescent protein; EGFP, enhanced GFP; GFP-Tg mice, C57BL6/Tg14 (act-EGFP) OsbY01 mice; HSC, hematopoietic stem cell; E, embryonic day; MSC, mesenchymal stem cells; MAPC, multipotent adult progenitor cell.

☆☆ This work was supported by Grants-in-Aid for Scientific Research from the Japan Society for the Promotion of Science (No. 13470121 to Shuji Terai, Isao Sakaida, and Kiwamu Okita, and No. 13770262 to Shuji Terai) for translational research from the Ministry of Health, Labor and Welfare (H-trans-5 to Shuji Terai, Isao Sakaida, Hiroshi Nishina, and Kiwamu Okita).

* Corresponding author. Fax: +81-836-22-2240.
E-mail addresses: terais@yamaguchi-u.ac.jp (S. Terai), nishina@mol.f.u-tokyo.ac.jp (H. Nishina).
[1] Request for Anti-Liv8 contact to Dr. Hiroshi Nishina, Department of Physiological Chemistry, Graduate School of Pharmaceutical Science, University of Tokyo, Hongo 7-3-1, Bunkyoku, Tokyo 113 0033, Japan.

0006-291X/$ - see front matter © 2003 Published by Elsevier Inc.
doi:10.1016/j.bbrc.2003.12.044

BMC has been an attractive cell source in regenerative medicine because getting BMC is easier than obtaining other tissue-specific stem cells [7].

However, the results of recent studies have been mixed in that some studies found that BMC was hardly transdifferentiated while others documented high levels of transdifferentiation [8,9]. Successful transdifferentiation in cell therapy involves various cell and recipient factors, and these factors interact in a complex manner. Therefore, it is difficult to identify the conditions necessary for transdifferentiation, contributing to the varied results among past studies. A past study using a fumarylacetoacetate hydrolase (FAH) knockout mice (metabolic tyrosinemia model) showed that hepatic functions could be compensated by transplanting Lin-Kit + Sca + Thy1low (KTLS) marrow cells [10]. In the FAH model, KTLS cells form foci and transdifferentiate into hepatocytes. Results of recent studies suggest that KTLS cells transdifferentiate into hepatocytes due to fusion with hepatocytes [11,12]. The FAH model is a specialized model of metabolic liver damage, making it possible to analyze the transdifferentiation of BMC into hepatocytes and functional compensation. However, a model with which the transdifferentiation of BMC can be analyzed under conditions of more general liver damage is needed. Using autologous transplantation in GFP transgenic mice [13], we established an isogenic transplantation model to assess the transdifferentiation of BMC into hepatocytes. This model is unique in that uncultured BMCs efficiently migrate into the peri-portal area of the liver and transdifferentiate into immature hepatoblasts and differentiate into mature hepatocytes under the specific "niche" of persistent liver damage induced by persistent intraperitoneal administration of carbon tetrachloride (CCl_4) [14]. In this model, liver cirrhosis was induced by 4 weeks CCl_4 injection, and BMCs isolated from GFP transgenic mice were transplanted through the caudal vein. It is possible to chronologically observe colonization and transdifferentiation of BMC in the liver by continuous administration of CCl_4, and we have named this model as the "GFP/CCl_4 model." Furthermore, in this model, as in the natural development of the liver, BMCs appear to be transdifferentiated into hepatoblasts and then into hepatocytes. In our GFP/CCl_4 model, the timing of cell transplantation and the state of recipients appear to be suitable for the transdifferentiation of BMC into hepatocytes. Cell transplantation and continuous liver damage made efficient transdifferentiation of BMC into hepatocytes. In a system similar to ours, human hematopoietic stem cells (HSCs) were transplanted into the bone marrow of immunologically tolerant NOD/SCID mice before administration of CCl_4, and these cells differentiated into albumin-positive hepatocyte-like cells after the CCl_4 administration [15]. These findings suggest that a special "niche" created by CCl_4-induced liver damage is important for the migration of BMC to the liver and transdifferentiation into hepatocytes. Also, it has been reported recently that CCl_4 administration is effective for improving the colonization of HSC to liver of NOD/SCID [16].

The liver functions as a metabolic organ, but during the fetal period, from embryonic day (E) 12 to 16 (E12–E16), the liver functions as a hematopoietic organ [17]. Several studies have reported that mesenchymal cells affect hepatic hematopoiesis during the fetal period [18,19]. After this hematopoietic period, hepatoblasts are involved in a complex manner to develop the liver as a metabolic organ. However, documentation of the existence of HSC in the adult liver suggests that, even in the adult liver, blood cells and hepatocytes still play some role in the maintenance of hepatic function [20]. To further analyze this aspect, we prepared new rat monoclonal antibodies using the fetal liver on E 11.5 as an antigen. One of these antibodies, anti-Liv2, specifically recognizes hepatoblasts in the fetal liver from E 9.5 to 12.5. The results of past studies using the anti-Liv2 antibody have shown that SEK1, a stress-signaling kinase, plays an important role in the proliferation of hepatoblasts, thus suggesting that inflammatory signals are involved in the proliferation of hepatoblasts [21].

Although various theories explain the existence of pluripotent stem cells in BMC, the exact composition of stem cells in BMC is not clear at this time; the following cell types are known to exist in bone marrow: HSC [4,10], side population cells [22], and mesenchymal stem cells (MSC) [23]. Although past studies used the existing antibodies and techniques, there have not been any studies based on the findings associated with natural liver development. Using fetal liver as an antigen, we prepared a new monoclonal antibody, anti-Liv8 antibody, to analyze which subpopulation of BMC could differentiate into hepatocytes under CCl_4-induced continuous liver damage in the GFP/CCl_4 model [14]. This anti-Liv8 antibody recognizes hematopoietic cells using a specific cell surface marker and it can be used to separate cells. In the present study, we used this new antibody to separate BMC of adult mice and then transplanted the different types into mice under identical conditions of the GFP/CCl_4 model to ascertain which types of BMCs transdifferentiate into hepatocytes.

Materials and methods

Mice. C57BL6/Tg14 (act-EGFP) OsbY01 mice (GFP-Tg mice) showed GFP expression in multiple tissue and cells and were kindly provided by Masaru Okabe (Genome Research Center, Osaka University, Osaka, Japan) [13]. C57BL/6 female mice were purchased from Japan SLC (Shizuoka, Japan). AML1 knockout mice were generated

as described previously [24]. The genetic background of these mice used in this study was C57BL/6 mice. Male and female mice were mated overnight and female mice were scored based on varginal plaques taken to represent E 0.5. Mice were anesthetized at the completion of experiments. All processes, including surgical steps, were undertaken with the guidance of the committee for animal and recombinant DNA experimentation at Yamaguchi University.

Production of rat monoclonal antibody, Liv8. Eight-week-old WKY/NCrj female rats were immunized in the hind footpads with 100 μg E 11.5 murine fetal liver lysate in complete Freund's adjuvant (0.2 ml). Anti-Liv8 antibodies were raised according to a previously described protocol [21].

Immunohistochemical staining for fetal liver. Fetal liver at E11.5 was obtained from c57/BL/6 mice and AML1 knockout mice. Tissue preparation and immunohistochemical analysis were performed according to a previously described protocol [21]. We analyzed anti-Liv2- and anti-Liv8-positive cells in fetal liver.

Preparation of GFP-positive BMC. For isolation of BMC, GFP-Tg mice were sacrificed by cervical dislocation and the limbs were removed. GFP-positive BMCs were flushed from the medullary cavities of tibias and femurs with PBS culture solution using a 25 G needle. The cell solution was filtered through a cell strainer (16 μm) to remove particular matter and centrifuged at 500*g* for 5 min. After centrifugation, the supernatant was removed and cells were resuspended to prepare 1.0×10^6 cells/ml GFP-positive BMC solutions. Preparation of BMC takes approximately 1.5 h.

FACS analysis of BMC using Liv8 antibody. Prepared GFP-positive BMCs were reacted with rat biotin anti-Liv8 IgG antibody, R-Phycoerythrin (R-PE)-conjugated rat anti-CD45 (leukocyte common antigen) monoclonal antibody (PharMingen, San Diego, USA) at the rate of 1 μg per 10^6 total cells, mixed well, and incubated in the gobos for 30–40 min at 4 °C. Following the incubation with the first antibody, the cells were washed twice by 0.02 M PBS and centrifuged at 500*g* for 5 min. Labeled cells were then reacted to streptavidin–fluorescein isothiocyanate (FITC) conjugate (PharMingen) at the rate of 1 μg per 10^6 total cells, mixed well, and incubated in the gobos for 30–40 min at 4 °C. After that, these were washed out once with 0.02 M PBS and centrifuged at 500*g* for 5 min. The labeled cells were analyzed using FACS Calibur (Becton–Dickinson).

Sort GFP positive BMC by Liv8 antibody. Prepared BMCs were reacted to rat anti-Liv8 IgG antibody at the rate of 1 μg per 10^6 total cells, mixed well, and incubated in the gobos for 30–40 min at 4 °C. Then cells were washed two times by 0.02 M PBS and centrifuged at 500*g* for 5 min. Cells were labeled with rat anti-Liv8 IgG antibody by reacting with Goat Anti-Rat IgG MicroBeads (Miltenvi Biotec GmbH, Bergisch Gladbach, Germany) at the rate of 20 μl per 10^7 total cells, mixed well, and incubated for 20–30 min at 4 °C. Labeled cells were washed once by 0.02 M PBS and centrifuged at 500*g* for 5 min. These cells were separated into Liv8-positive cells or negative cells by the Auto Magnetic Cell Sorting system (Auto MACS) (Miltenvi Biotec GmbH) for 10 min per tube.

Transplantation of Liv8-positive or negative BMC into persistent liver damaged mice. We developed a new in vivo model "GFP/CCl_4 model" for monitoring differentiation of BMCs into hepatocytes [14]. To generate a liver damage group, 0.5 ml/kg of CCl_4 was injected into the peritoneum of 6-week-old C57BL/6 females twice a week for 4 weeks. Liver cirrhosis resulting from the continuous injections of CCl_4 was confirmed. A control group of C57BL/6 mice that had not been treated with CCl_4 was also used. One day after the eighth injection, sorted Liv8-positive or Liv8-negative BMC (1×10^5 cells) was slowly injected into the caudal tail vein of mice using a 31 G needle and a Hamilton syringe. After transplantation, CCl_4 injections (0.5 ml/kg) were continued twice a week. Mice were sacrificed weekly up to 4 weeks.

Tissue preparation. The livers were thoroughly perfused via the heart with 4% paraformaldehyde (Muto, Tokyo, Japan). This step was crucial for washing out contaminating blood cells. For fixation, the perfused livers were incubated with 4% paraformaldehyde (Muto) overnight and then soaked in 30% sucrose for a few more 3 days. Tissues were frozen in dry ice and then sectioned into 18-μm slices using a cryostat (Moriyasu Kounetsu, Osaka, Japan) in preparation for dyeing.

Immunohistochemistry and double immunofluorescence for GFP. To avoid autofluorescence, we used immunostaining to assess the expression of GFP. Cells expressing GFP were analyzed by both fluorescent microscopy and conventional immunohistochemistry with anti-GFP antibody (Santa Cruz Biotechnology, Santa Cruz, California, USA). Immunohistochemical analysis was performed according to a previously described protocol [14,25]. Sectioned tissues were incubated with anti-GFP antibody (1:5000 FL, sc-8334; Santa Cruz Biotechnology), anti-albumin (1:5000, 55462; ICN Pharmaceuticals, Costa Mesa, CA, USA), and anti-Liv2 antibody (1:5000) [21]. For fluorescence immunohistochemistry, tissues were incubated with Alexa Fluor R 488 and 568 donkey anti-goat IgG(H + L) conjugate, Alexa Fluor R 488 goat anti-rabbit IgG(H + L) conjugate, and Alexa Fluor R 568 goat anti-rat IgG(H + L) conjugate (Molecular Probes, Eugene, OR) as secondary antibodies. Positive cells in the liver were quantified using a Provis microscope (Olympus, Tokyo, Japan) equipped with a charge coupled devise (CCD) camera and subjected to computer-assisted image analysis with MetaMorph software (Universal Imaging, Downingtown, PA). A total of 10 different areas per liver section were analyzed independently and the areas of positive cells were calculated using the MetaMorph software.

Serum albumin level analysis. Serum albumin levels during the 4 weeks after Liv8-positive or Liv8-negative BMC transplantation were analyzed using the SPOTCHEM EZ SP-4430 dry chemical system (Arkray, Kyoto, Japan).

Statistical analysis. Values are shown as means ± SE. Data were analyzed by analysis of variance with Fisher's projected least significant difference test.

Results

Anti-Liv8 antibody detected hematopoietic progenitor cell in fetal liver at E 11.5

Previously we had raised a rat monoclonal antibody, anti-Liv2, which recognized hepatoblasts at E 9.5 [21]. As shown in Fig. 1A, Liv2-positive cells were also detected in fetal liver at E 11.5. Using the antibody developed in this study, Liv8-positive cells were seen in the fetal liver on E 11.5 (Fig. 1B). Fetal liver at E 11.5 functions as a secondary hematopoietic organ [17]. We analyzed whether anti-Liv8 positive cell is associated with hepatoblast or hematopoietic cell. We found Liv2-positive cells (Fig. 1C), but no Liv8-positive cells (Fig. 1D), in the fetal liver of $AML1^{-/-}$ embryos which do not undergo definitive hematopoiesis [24]. These results suggested that anti-Liv-8 recognizes hematopoietic progenitor cell in fetal liver.

Liv8-positive cells exist in adult bone marrow and express CD45

Next, we investigated Liv8-positive cells in the BMC of adult GFP Tg mice. Liv8-positive cells were found to be present among adult BMCs in adult bone marrow when analyzed in GFP-Tg mice. We found around 32%

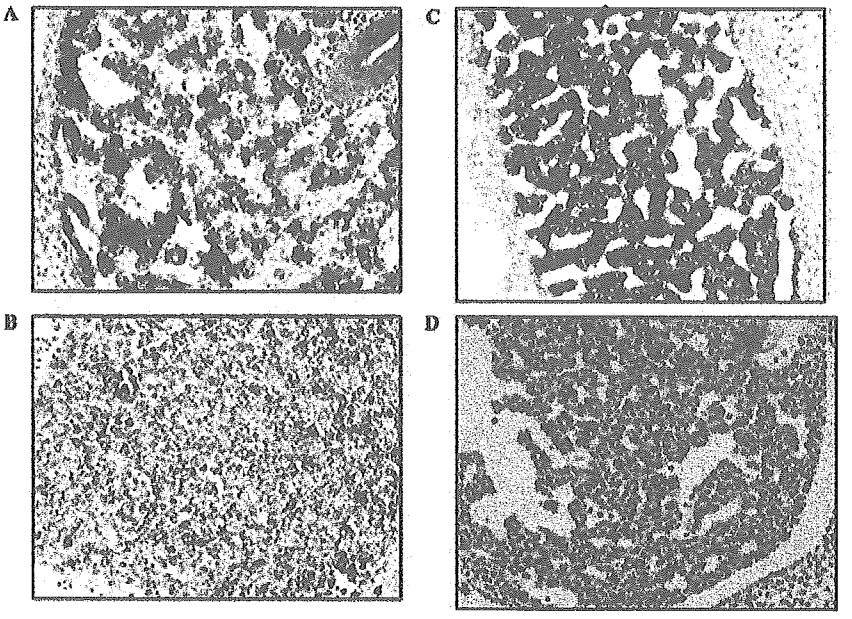

Fig. 1. (A–D) Liv2 and Liv8 expression at E 11.5 in normal and AML$^{-/-}$ mice. Liv2 (A,C) and Liv8 (B,D) expression at E 11.5 in normal fetal liver (A,B) and AML$^{-/-}$ mice (C,D). Magnification: (A–D) at 200×.

of Liv8-positive cells in adult GFP-Tg mice (Fig. 2A). We also analyzed the relationship between Liv8 and CD45, and found that 54% of Liv8-positive cells also expressed CD45 (Fig. 2B). These results showed that anti-Liv8 is useful to separate hematopoietic cell and non-hematopoietic cell.

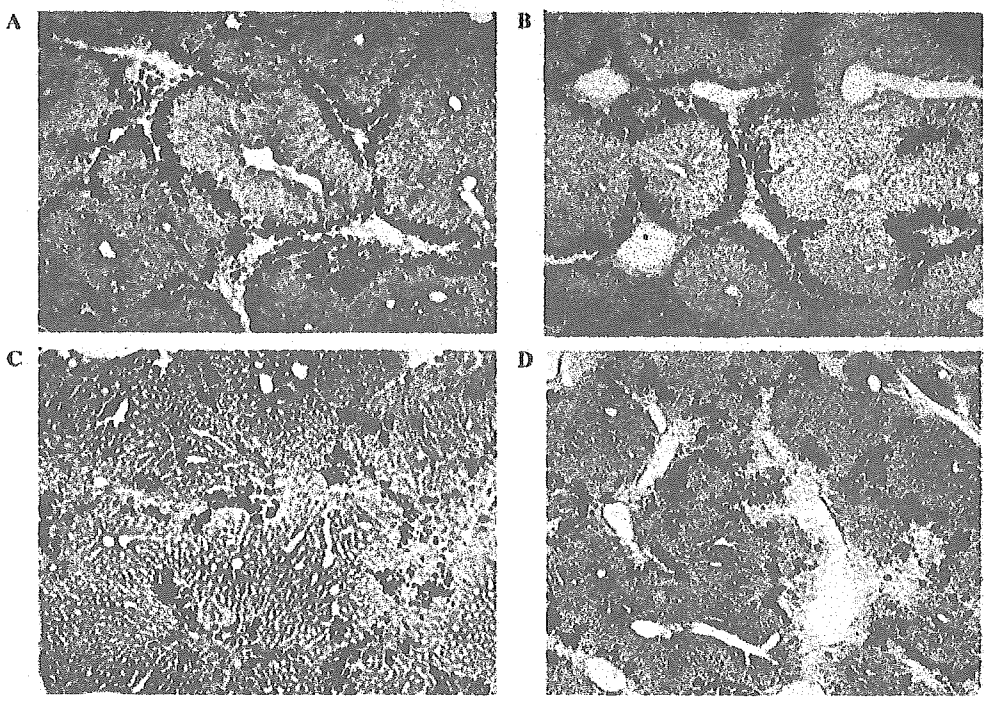

Fig. 3. (A–D) Expression of GFP in liver after transplantation of Liv8-positive and Liv8-negative cells. GFP expression in the liver after transplantation of Liv8-positive BMCs at 1 week (A) and 4 weeks (C), GFP expression at the liver after Liv8-negative BMC transplantation at 1 week (B) and 4 weeks (D) after cell injection. Magnification 200×.

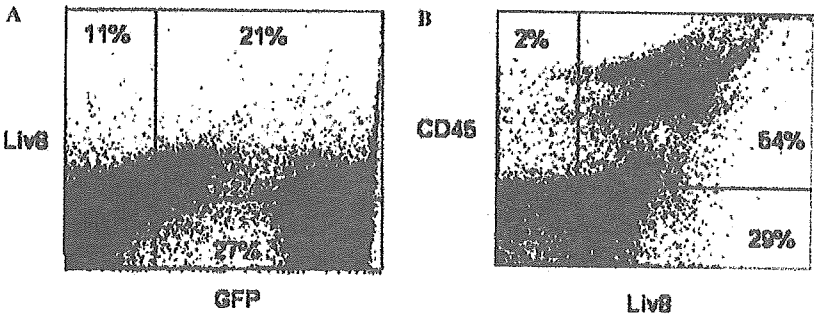

Fig. 2. Expression of CD45, Liv8 in bone marrow cell. FACS analysis of all BMCs of GFP-Tg mice. (A) Staining with Liv8 and GFP. (B) Staining with CD45 and Liv8.

Liv8-negative cells repopulated at the liver more than Liv8-positive cells

After separating Liv8-positive cells from Liv8-negative cells using AutoMACS, these cells were transplanted to recipient mice with CCl_4-induced liver cirrhosis. At one week after transplantation, both Liv8-positive (Fig. 3A) and Liv8-negative cells (Fig. 3B) colonized around the portal vein, with no marked differences in the rate of colonization (Table 1). In the Liv8-positive cell transplanted group, the number of GFP-positive cells in the liver increased transiently, but at four weeks after transplantation, the number of GFP-positive cells was significantly lower in the Liv8-positive cell group (Fig. 3C) than in the Liv8-negative cell group (Fig. 3D). Furthermore, GFP-positive cells were colonized inside the hepatic lobes in the Liv8-negative cell group at four weeks after transplantation. These results showed that Liv8-negative cell repopulated more than Liv8-positive cell.

The Liv8-negative cells transdifferentiate into hepatoblast phenotype

We showed in previous studies that transplanted BMCs transdifferentiate into Liv2-positive hepatoblasts and then further differentiate into hepatocytes [14,21]. In the present study, we also investigated the presence of cells expressing Liv2. Liv2-positive cells were identified by immunostaining, and the results showed that Liv2-positive cells were seen around the portal region one week after transplantation, but that there was no significant difference in the number of Liv2-positive cells between Liv8-positive and Liv8-negative cell groups (Figs. 4A and B, and Table 1). With time, the number of Liv2-positive cells in the liver decreased significantly for the Liv8-positive cell group (Figs. 4C and D and Table 1). The transdifferentiation of myelogenic GFP cells into Liv2 cells was investigated. Cells that expressed both Liv2 and GFP were detected at four weeks after transplantation, and fluorescent staining showed that the expression of Liv2 by myelogenic cells was higher for the Liv8-negative cell group (Figs. 4E and F). These results indicated that Liv8-negative cell could be transdifferentiated into hepatoblast phenotype.

Albumin expression in the liver and serum albumin level following transplantation of Liv8-positive and Liv8-negative BMCs

At one week after cell transplantation, there was no marked change in the expression of albumin for both Liv8-positive and Liv8-negative cell groups (Figs. 5A and B). However, at four weeks after transplantation, the expression of albumin decreased with time for the Liv8-positive cell group (Fig. 5C), but remained the same for the Liv8-negative cell group (Fig. 5D). Furthermore, at four weeks after cell transplantation, the number of yellow cells expressing both albumin and GFP was higher for the Liv8-negative cell group (Figs.

Table 1
Percent of area for each differentiation marker after Liv8(+) and Liv8(−) cell transplantation under the persistent liver damage

		1 week ($n = 5$)	2 weeks ($n = 5$)	3 weeks ($n = 5$)	4 weeks ($n = 5$)
GFP	Liv8(+)	11.1 ± 1.7	15.1 ± 2. 1	9.4 ± 0.8	5.1 ± 0.6*
	Liv8(−)	11.7 ± 1.0	13.2 ± 0.8	12.4 ± 2.6	9.5 ± 3.6*
Liv2	Liv8(+)	6.0 ± 1.1	7.3 ± 3.5	8.2 ± 1.8	3.3 ± 0.9
	Liv8(−)	5.5 ± 1.3	5.8 ± 0.8	9.2 ± 0.6	7.7 ± 0.9
Albumin	Liv8(+)	15.0 ± 1.9	14.9 ± 2.5	6.8 ± 2.6*	3.7 ± 1.4*
	Liv8(−)	12.7 ± 3.2	12.5 ± 3.2	14.8 ± 1.3*	10.6 ± 2.1*

Values shown are percent of the area occupied. * showed significant differences at each sampling point ($n = 5$) at $p < 0.05$ between Liv8(+) and Liv8(−) cell transplantation groups.

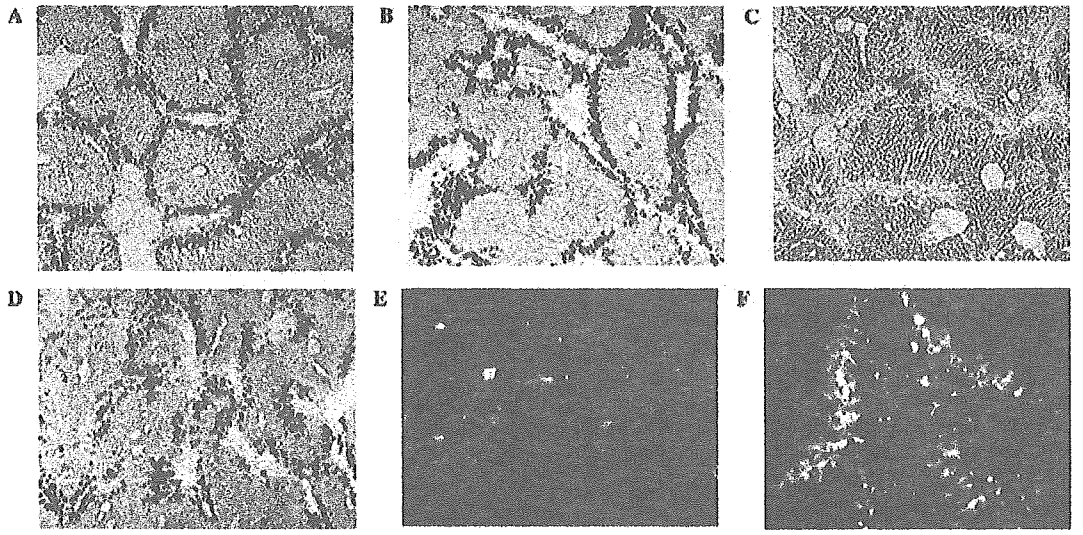

Fig. 4. (A–F) Expression of Liv2 antigen in liver after transplantation of Liv8-positive and Liv8-negative cells. Liv2 antigen expression at 1 week (A) and 4 weeks (C) after Liv8-positive BMC transplantation. Magnification at 200×. Liv2 antigen expression at liver at 1 week (B) and 4 weeks (D) after Liv8-negative BMC transplantation. Double fluorescent staining (red, Liv2; green, GFP; and yellow, Liv2 & GFP) of the liver at 4 weeks after Liv8-positive cell transplantation (E) and Liv8 negative cell transplantation (F) Magnification: (A–D) 200×, (E,F) 400×.

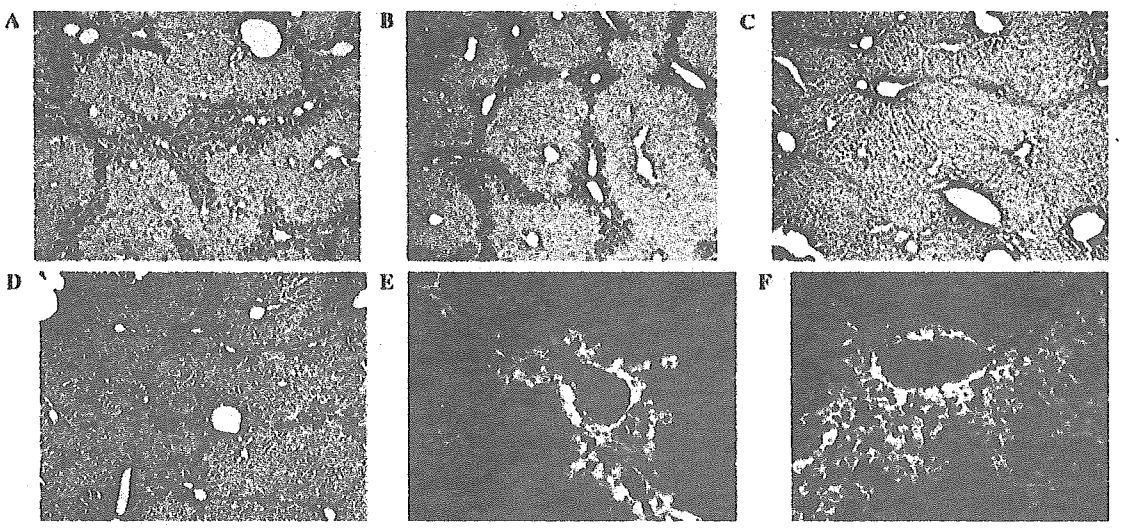

Fig. 5. (A–L) Expression Albumin after transplantation of Liv8-positive and Liv8-negative cells. Albumin expression at 1 week after transplantation of Liv8-positive cells (A) and Liv8-negative cells (B). Albumin expression at 4 weeks after transplantation of Liv8-positive cells (C) and Liv8-negative cells (D). Double fluorescent staining (red, albumin; green, GFP; and yellow, albumin & GFP) of liver at 4 weeks after transplantation of Liv8-positive cells (E) and Liv8-negative cells (F). Magnification: (A–D) 200×, (E,F) 400×.

5E and F). To ascertain whether transplanted cells were functioning as hepatocytes, serum albumin levels were measured. Serum albumin levels increased for both groups and were higher for the Liv8-negative cell group than the Liv8-positive cell group. The serum albumin levels at 4 weeks after Liv8-negative BMC transplantation showed the significantly higher levels for Liv8-negative cell group compared to the Liv8-positive BMC group ($n = 5$, $p < 0.05$) (Fig. 6). These results also showed that Liv8-negative cell could transdifferentiate into albumin-positive hepatocyte.

Discussion

The anti-Liv8 antibody is a useful antibody to separate hematopoietic cells and non-hematopoietic cells in adult bone marrow. We found Liv8-positive cells in fetal